

**ENGINEERING SCAFFOLD-FREE DENTAL ORGANOIDS
USING HUMAN STEM CELLS FROM THE APICAL PAPILLA (SCAP)**

by

Nadeen Mahmoud Meshry

BDS, Alexandria University, 2016

Submitted to the Graduate Faculty of the
School of Dental Medicine in partial fulfillment
of the requirements for the degree of
Master of Science

University of Pittsburgh

2021

UNIVERSITY OF PITTSBURGH

SCHOOL OF DENTAL MEDICINE

This thesis was presented

by

Nadeen Mahmoud Meshry

It was defended on

July 14, 2021

and approved by

Dr. Elia Beniash, PhD, Professor Chair, Department of Oral and Craniofacial Sciences

Dr. Juan Taboas, PhD, Associate Professor, Department of Oral and Craniofacial Sciences

Thesis Advisor: Dr. Fatima N Syed-Picard, Assistant Professor, Department of Oral and
Craniofacial Sciences

Copyright © by Nadeen Mahmoud Meshry

2021

**Engineering Scaffold-free Dental Organoids
Using Human Stem Cells from the Apical Papilla (SCAP)**

Nadeen Mahmoud Meshry, BDS, MS

University of Pittsburgh, 2021

ABSTRACT

The clinical dilemma of treating immature necrotic teeth has been the driving force behind the field of regenerative endodontics. Through evoking bleeding from the periapical tissues, clinicians have noticed root elongation and closure following this treatment. The periapical location of the apical papilla tissue renders it a very probable source of some of the progenitor cells that are homed to the canal space during this procedure. This study aims to generate an experimental model for studying the regenerative capacity of the apical papilla tissue, through engineering scaffold-free dental organoids (SFDO) using human stem cells from the apical papilla (SCAP).

The SFDOs were generated by culturing human SCAP to form a cell sheet, which later contracts resulting in the formation of a 3D construct which was cultured in osteogenic medium for 14 days before analyzing the results. Hematoxylin-and-Eosin-stained histological sections of the SFDOs revealed a densely cellular structure, with two distinct morphologies; spindle-shaped peripheral cells and distinctly more rounded cells in the center. Alizarin red staining for calcium deposition showed that the organoids had a triple mineralization pattern, with (1) an outermost thin rim of unmineralized tissue (corresponding to the flat peripheral cells) that encloses (2) a mineralized intermediate zone, which in turn exhibits a decreasing gradient of mineralization that ends with (3) an innermost core of unmineralized tissue. The resultant multi-tissue structure potentially resembles the organization seen in a tooth root (outer PDL, intermediate cementum/dentin, inner pulp). Immunofluorescent staining showed that expression of DSP (a dentinogenic marker) and asporin (a reported PDL marker) were localized to the inner bulk and the peripheral part of the SFDO respectively.

These results suggest that SCAP could have the potential to regenerate a full tooth root-like structure. As such, SCAP might be worth exploration as a potential cell-based endodontic treatment modality for promoting root elongation in cases of immature necrotic teeth.

Table of Contents

ABSTRACT	v
ACKNOWLEDGMENTS	xi
1.0 INTRODUCTION	1
1.1 Tooth anatomy and development	1
1.2 The clinical challenge of treating necrotic teeth with under-developed roots	3
1.3 Stem/progenitor cell populations inside the oral cavity	7
1.4 Possible role of SCAP among the dental cell populations driving root elongation in revascularized immature teeth	9
1.5 Why scaffold-free tissue engineering?	10
2.0 HYPOTHESIS	13
3.0 MATERIALS AND METHODS	14
3.1 Apical papilla cell isolation, expansion and storage	14
3.2 Confirmation of osteogenic potential of the isolated SCAP	15
3.3 Engineering of the 3D organoids	16
3.4 Histological characterization of the engineered 3D SCAP constructs	19
3.4.1 Hematoxylin and Eosin stain	19
3.4.2 Alizarin Red S stain	20
3.4.3 Immunostaining	20
3.5 Fourier-transform infrared spectroscopy (FTIR)	22
4.0 RESULTS	23
4.1 Morphology and osteogenic differentiation capacity of SCAP	23

4.2 Generating the 3D SCAP organoids	25
4.3 Histological evaluation of tissue morphology and mineral deposition in the SCAP constructs.....	27
4.4 Fourier-transform infrared spectroscopy (FTIR) analysis	32
4.5 Evaluation of protein expression in the SCAP constructs	33
5.0 DISCUSSION	36
6.0 CONCLUSION	47
Appendix A Protein expression in SCAP organoids at one week.....	48
Appendix B Implanting the SCAP organoids in vivo	49
Appendix B.1 Materials and methods	49
Appendix B.2 Results	51
Bibliography	53

List of Tables

Table 1 Primary antibodies.....	21
Table 2 Secondary antibody.....	22

List of Figures

Figure 1 Illustration showing cross-section of an adult human molar	2
Figure 2 Light micrograph showing bell stage of tooth development.....	3
Figure 3 Anatomy and histology of the apical papilla.....	8
Figure 4 Isolation, culture and osteogenic differentiation of SCAP.....	24
Figure 5 Experimental design of the study	25
Figure 6 Engineering the dental organoids from SCAP.....	26
Figure 7 Histological analysis of SCAP organoids at one week.....	29
Figure 8 Histological analysis of SCAP organoids at two weeks	31
Figure 9 FTIR spectroscopy graph	32
Figure 10 Protein expression analysis of SCAP organoids	34
Figure 11 Histological analysis of DPC organoids.....	38
Appendix Figure 1 Immunofluorescent staining of SCAP organoids at one week.....	48
Appendix Figure 2 Histological analysis of SCAP explants.....	52

ACKNOWLEDGMENTS

First and foremost, all thanks and praise is due to Allah, the most Gracious, the most Merciful, Creator of the heavens and earth, and my Creator and Sustainer. I thank Allah for enabling me to undertake my master's research at the University of Pittsburgh and for His innumerable blessings upon me.

I would then like to thank my master's advisor Dr. Fatima Syed-Picard for letting me be part of her lab and for providing continuous support and advice to me throughout my two years in the program. I appreciate everything she has done for me really and will always be grateful to her.

I would also like to express my warmest gratitude to Kristi Rothermund, for teaching me the techniques used in the lab & for being patient with me & generous with both her time & effort.

I would also like to thank my thesis committee members Dr. Elia Beniash and Dr. Juan Taboas for agreeing to be part of my committee and for offering guidance and support to finish my project. I would like to specially thank dr. Elia Beniash for his time and effort in helping me with FTIR for my project. And I would like to thank dr. Juan Taboas for being generous with his time and patient with all my question in our class "Foundations in modern laboratory methods". It was truly one of the most beneficial courses I've taken here and I have learned a lot from this class.

I am also very grateful to our sessions in Journal Club, which have helped me develop a better understanding of research articles and how to navigate through them. I would like to thank Dr. Dobrawa Napierala for managing this class and providing us with a safe environment to learn and ask questions and room to grow as critical thinkers. I am truly fortunate to have been part of the Oral Biology program. I learned so much during my time here.

I also want to thank my friends in the lab Michelle Drewry & Tia Calabrese for being such great friends & for their support and help through rough times. I would like to thank all my friends in the program & in school: Rutuja, Taiana, Arwa, Catherine, Mairobys & a special thanks to Nadine Robert for being such a kind friend to me. I am fortunate to have known each & every one of my friends here. They have all helped me feel home away from home in their own special way.

I would like to gratefully acknowledge Fulbright, for granting me this scholarship to earn my master's degree here in the U.S.

Last, but certainly not least, I would like to express my everlasting gratitude to my family: my mother, my sister and my brother who have been with me through it all. And a special thank you to my beloved father Mahmoud Meshry who passed away last September. My dad was the one who taught me English and sang to me the English alphabet when I was young. And here I am today. He was truly an amazing dad and I owe everything that I am today to him and my mother, after God. May Allah's peace and mercy befall him...

1.0 INTRODUCTION

1.1 Tooth anatomy and development

Though a seemingly simple and basic organ, a tooth has proven to be anything but simple or basic. Our current understanding of how a tooth forms, the complexity of its anatomic layers and the means by which it is anchored to the surrounding bone makes the task of mimicking such a complex structure extremely difficult. From an anatomic perspective, a tooth is comprised of a coronal portion (crown) and a root portion (root). At its core, the tooth harbors a soft, innervated and vascularized tissue known as “the pulp”. Encasing the pulp tissue is “dentin”, which is the mineralized structure that forms the main bulk of the tooth. Both pulp and dentin are often collectively referred to as the dentin/pulp complex (Fig.1). In the coronal part of the tooth, dentin is covered by a hard mineralized tissue known as enamel; whereas in the root, it is covered by another mineralized tissue (much less hard than enamel) known as cementum. In the oral cavity, teeth reside inside holes within the alveolar bone –known as tooth sockets– and are anchored to the alveolar bone via a soft tissue structure known as periodontal ligament. The periodontal ligament (PDL) is a structure of predominantly specialized connective tissue fibers that serves to anchor the tooth to the alveolar bone and preserve its integrity by steadily dissipating the occlusal forces that the tooth withstands unto the surrounding bone⁽¹⁾. The anatomy and orientation of PDL fibers enables them to perform their function exceptionally well, where the fibers are embedded into the alveolar bone on one end, and into cementum on the other end. Collectively, cementum, PDL and bone, along with the gingival tissue surrounding the tooth, form what is known as “the periodontium”⁽¹⁾.

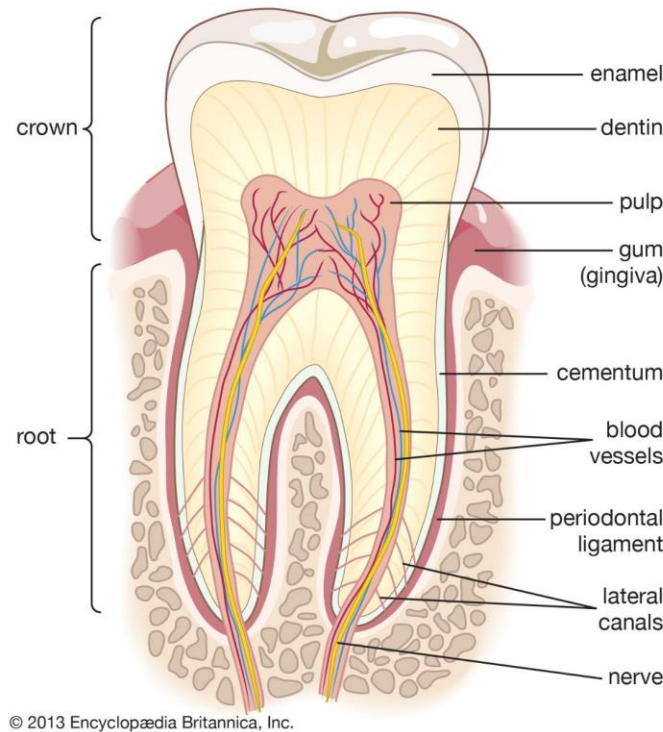


Figure 1 Illustration showing cross-section of an adult human molar (Image from from Encyclopædia Britannica)⁽²⁾

During tooth development, the dentin/pulp complex differentiates from an ectomesenchymal tissue known as the dental papilla (Fig.2). This structure gives rise to the dentin/pulp complex through differentiating into the pulp and giving rise to the odontoblasts, which in turn secrete the dentin matrix. Another important ectomesenchymal tissue is a structure known as dental follicle or dental sac. This tissue is also in the form of ectomesenchymal condensation (but relatively more fibrous than the dental papilla) and it encircles both the enamel organ and the dental papilla (Fig.2).

With regard to the differentiation of the dental papilla, it has been established that in the crown, cells of the inner enamel epithelium (shown in Fig.2) induce the odontoblastic differentiation of the cells of the dental papilla⁽¹⁾. Similarly in the root, as Hertwig's epithelial root sheath (a double epithelial layer, derived from the inner and outer enamel epithelium) extends

apically, it initiates the odontoblastic differentiation of the dental papilla cells to form the dentin/pulp complex of the root portion of the tooth⁽¹⁾. This has given great weight to the pivotal role of the dental papilla in development of the dentin/pulp complex. As a result, researchers embarked on a search for any possible remnants of this tissue in the oral cavity of patients, to be used for regenerative studies that aim at recapitulating the events of development to ideally regenerate this major component of the tooth – the dentin/pulp complex.

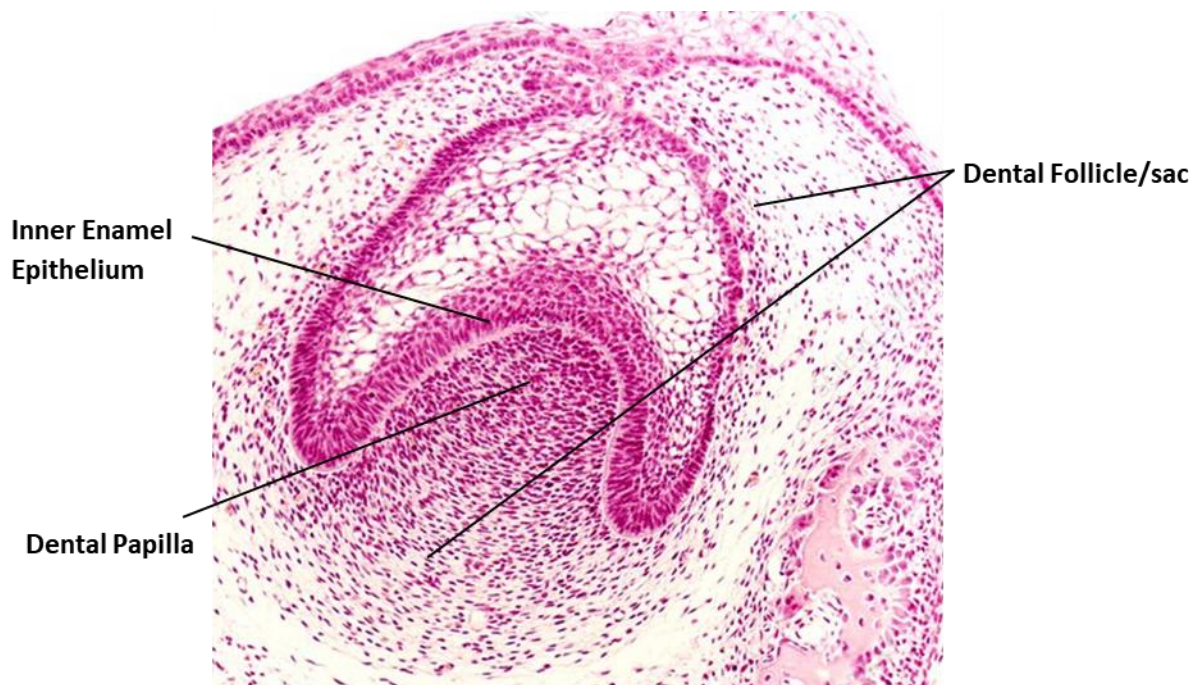


Figure 2 Light micrograph showing bell stage of tooth development(Image from Science Photo Library)⁽³⁾

1.2 The clinical challenge of treating necrotic teeth with under-developed roots

Ideally, a newly erupted tooth matures normally, taking approximately three years to complete its root development following its eruption. However, a clinical dilemma arises if the

sequence of normal root maturation is disrupted. When an immature permanent tooth sustains trauma or endodontic/periapical infection that causes pulp necrosis, clinicians face the problem of endodontically-treating these teeth. This is because immature permanent teeth have wide apices and thin dentinal walls; where the former jeopardizes the integrity of apical seal while the latter renders the tooth prone to fracture after mechanical instrumentation and debridement of the dentinal wall. In addition, the inadequate crown/root ratio negatively affects the prognosis of these teeth. As a result, conventional root canal therapy is deemed inappropriate for such cases and consequently, alternative treatment techniques have been in demand.

One approach, known as apexification, involves building a calcified barrier apically to provide initial apical closure followed by conventional endodontic filling of the canal space. Calcium hydroxide [Ca(OH)₂] was initially the material of choice for this procedure. However, mineral trioxide aggregate (MTA) has gained more favor among clinicians owing to its ease of handling and the shorter time needed for forming the calcified barrier⁽⁴⁾. This technique has been widely used in the clinic, as it overcomes the critical problem of attaining proper apical seal for underdeveloped roots. However, the thin dentinal walls and improper crown/root ratio are not addressed in this case, leaving apexified teeth subject to fracture. Indeed it has been reported that fracture is the leading cause of failure of MTA-apexified teeth⁽⁵⁾.

Clinicians have therefore contrived alternative treatment modalities that aim at revascularizing the canal space to allow for proper root elongation and closure, as this would allow the treated teeth to have a more adequate crown/root ratio that can safeguard against fracture failure. These have been generally referred to as Regenerative Endodontic Treatment (RET) techniques. These are typically done over two steps; where the first step entails proper canal disinfection followed by placement of an intracanal medicament (usually triple antibiotic paste) and sealing

coronally with a temporary filling, whereas the second step involves removal of the temporary filling and intracanal medicament, performing canal irrigation, followed by bypassing the canal space and poking at the apical tissues to induce bleeding (i.e. deliberate overinstrumentation) and finally closing over the blood clot by MTA⁽⁶⁾. The blood clot that fills the canal space acts as a scaffold that brings along progenitor cells and growth factors from the local environment of the developing root. This technique has shown clinical success in many cases, with symptoms eliminated, roots elongated, apices significantly narrowed and, in some cases, sensation restored⁽⁷⁻¹³⁾. However, the nature of the tissue that re-inhabits the root canal space remains largely unknown, with several reports of case-by-case variation⁽¹¹⁻¹³⁾. In fact, it would be safe to conclude that based on the available histological reports, a conventional dentin/pulp complex is not the typical outcome in these cases after all. The neo-formed tissue has been reported to be comprised of one or more of the following tissues and cells: fibrous connective tissue, cementum-like tissue, bone-like tissue, dentin-like tissue, intracanal “mineralized-islands”, odontoblast-like cells, “non-odontoblast-looking cells”, neurons and nerve fibers⁽¹²⁻¹⁴⁾. This has prompted some researchers to shy away from using the term “Regenerative Endodontics”, since repair rather than regeneration was the ultimate result of this approach. Alternative terms have included “Pulp Revascularization” as a more technically correct description of this approach, which is based on re-establishing vasculature of the root canal⁽¹⁵⁾. Others have gone further with drawing distinctions between the different terms and have favored the use of “Revitalization” as a distinctly more general term to describe the non-specific plethora of vital tissues that can re-inhabit the pulp canal space, rather than the impression of having only blood vessels formed, which the term “Revitalization” can mistakenly convey⁽¹⁶⁾. In spite of this, the term “Regenerative Endodontic Treatment” (RET) remains the most widely used term and a generally accepted one for describing this approach.

With such highly disorganized tissues re-inhabiting the canal space, an important concern would be to have mineralized tissues growing inside the root canal space. Intracanal calcifications are generally considered an unfavorable outcome, as these result in tooth discoloration and subsequent pulp necrosis if the condition advances to complete canal obliteration⁽¹⁷⁾. On another aspect, calcified canals can be clinically challenging to negotiate and debride when root canal therapy is needed. Common complications reported with endodontic treatment of such teeth include instrument fracture and canal perforation⁽¹⁸⁾. Considering the disorganized nature of the tissues that fill up the root canal space after RETs, it is then not at all surprising to find revascularization-associated intracanal calcifications (RAICs) a commonly reported finding for immature teeth that undergo RET. According to the literature review by Song et al⁽¹⁹⁾, which included 29 cases of RET, 62.1% of the cases developed RAIC. Of those cases, 72.2% had progressed to complete canal obliteration. And with the relatively short follow-up time after RET, it is possible that RAIC could be even more prevalent than what has been reported. This has prompted some researchers to call for larger studies with longer follow-ups to include RAIC as a common and unfavorable outcome to RET⁽²⁰⁾.

With yet another unsatisfactory outcome to the available treatments, more attention was diverted toward cell-based therapies. These therapies offer the advantage of knowing exactly the type of cells being introduced inside the canal and henceforth, having a more insightful prediction of the regenerative outcome.

1.3 Stem/progenitor cell populations inside the oral cavity

The search for stem/progenitor cell populations within the oral cavity proved to be worthwhile, yielding a generous surplus of eight different dental tissue-derived stem cell populations. Dental pulp stem cells (DPSCs) were the first to be isolated (Gronthos et al, 2000)⁽²¹⁾, followed by a rapid surge of the subsequently discovered populations: stem cells of human exfoliated deciduous teeth (Miura et al, 2003)⁽²²⁾, periodontal ligament stem cells (Seo et al, 2004)⁽²³⁾, dental follicle stem cells (Morsczeck et al, 2005), alveolar bone-derived stem cells (Matsubara et al, 2005)⁽²⁴⁾, stem cells from the apical papilla “SCAP” (Sonoyama et al, 2006)⁽²⁵⁾, tooth germ stem cells (Ikeda et al, 2006)⁽²⁶⁾ and gingival mesenchymal stem cells (Zhang et al, 2009)⁽²⁷⁾. For the purpose of regenerating the dentin/pulp complex (the main bulk of the tooth structure), derivatives of the dental papilla were the object of further investigation.

As the tooth develops, the dental papilla gradually loses some of its stem properties as it develops into a fully formed and mature dentin/pulp complex. Nonetheless, in 2000, Gronthos et al.⁽²¹⁾ were able to isolate a population of stem cells from fully formed and mature pulp tissue. These were given the name “Dental Pulp Stem Cells” (DPSCs) and have been shown to give rise to a dentin/pulp-like complex when transplanted subcutaneously, in mice, in conjunction with a mineral-inducing scaffold/carrier^(21, 28, 29). In addition, our group has shown that scaffold-less 3 dimensional constructs of dental pulp cells are able to self-organize into a dentin/pulp-like tissue in vitro and after subcutaneous transplantation, in mice, within a tooth root fragment⁽³⁰⁾.

In 2006, Sonoyama et al.⁽²⁵⁾ discovered a population of stem cells that reside in the soft tissue attached to the apical region of immature open-apexed roots. This tissue was found to be an apical extension of the dental papilla (seen in developing teeth) and was hence named “apical papilla”. Despite anatomically being a continuation of the dental pulp, histological findings

revealed a separation between the two tissues by a cell-rich zone⁽³¹⁾ (Fig.3). Furthermore, the apical papilla was found to harbor a population of stem cells different from those seen in the dental pulp. Stem cells of the apical papilla (SCAP) were found to possess some superior properties compared to DPSCs, namely faster proliferation rate, larger population doubling and greater migration ability^(25, 31, 32). These differences can potentially be attributed to the origin of both tissues; where DPSCs are isolated from mature tissue – that is the pulp (differentiated dental papilla), whereas SCAP are isolated from yet developing tissue – that is the apical papilla (undifferentiated papilla). Returning to the developmental role of the dental papilla, it follows that the apical papilla is the tissue that gives rise to the dentin/pulp complex of a developing root. It is then only natural that as the tooth root elongates and the apical foramen narrows down, the apical papilla tissue disappears and is no longer present when examining the roots of extracted fully mature close-apexed teeth. As such, SCAP isolated from the tissue of the apical papilla could be a proper cell source to regenerate the dentin/pulp complex of the yet-developing root of immature permanent teeth, and therefore, their regenerative capacity is worth exploring.

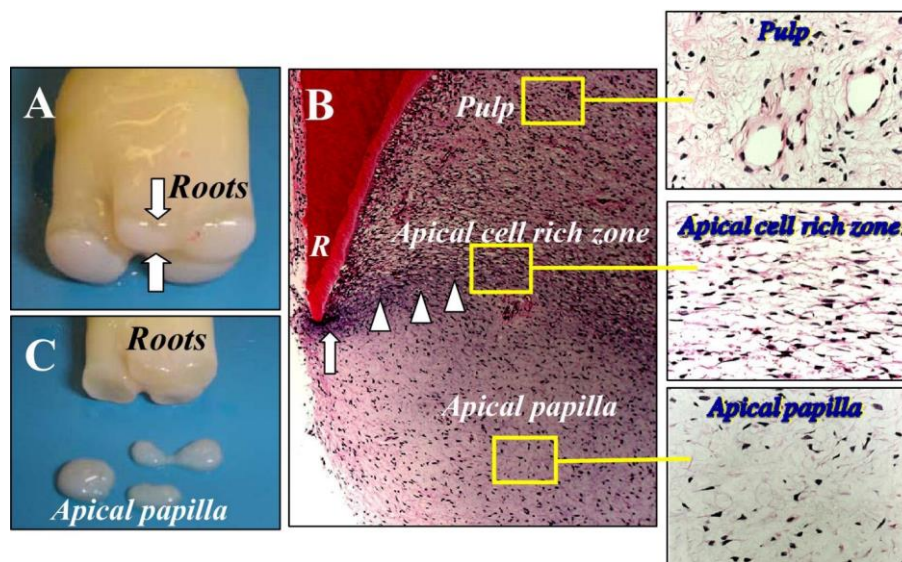


Figure 3 Anatomy and histology of the apical papilla (from Sonoyama et al. 2008)⁽³¹⁾

1.4 Possible role of SCAP among the dental cell populations driving root elongation in revascularized immature teeth

As previously mentioned, the nature of the regenerated tissues in revascularized root canals has been largely arbitrary, suggesting a more diverse tissue source than what was initially predicted. This is probably because in addition to what goes on during normal root elongation and closure, immature roots that have undergone RET have an important and game changing event – which is inflammation. Inflammatory cells are known to secrete a multitude of cytokines that can have a chemotactic effect on cell populations that otherwise would not have been recruited to the site of normal root development. In addition, inflammation in itself can alter the homeostatic nature of the cells recruited to the root canal space, pushing the progenitor cells down one path versus the other, thus resulting in an outcome that is aberrant to what would have been seen in case of a normally developing root. Perhaps as of yet, the identity of the contributing cell populations that re-inhabit the root canal has not been revealed as a matter of certainty, especially with the difficulty and ethical considerations related to obtaining histological samples of human teeth at different timepoints after receiving RET. However, based on the available histological records for these cases and knowledge of the anatomy of the tissues surrounding a developing root, the apical papilla, Hertwig's Epithelial Root Sheath (HERS), bone and periodontal ligament could all be involved in the process.

The anatomic location of the apical papilla renders it a very probable source of some of the progenitor cells that are homed to the canal space following overinstrumentation. In addition, the developmental role played by the dental papilla in forming a dentin/pulp complex qualifies the apical papilla tissue as an important, if not a key, player in this process. This hypothesis has been further substantiated when root development was hampered after surgical removal of the apical

papilla in a minipig model (Huang et al, 2008)⁽³³⁾. However, it has been suggested that since Hertwig's Epithelial Root Sheath (HERS) is what initiates the odontoblastic differentiation of the dental papilla during the events of normal root development, it is possible that it is the removal of HERS and not the removal of the apical papilla per se that hindered root development in this case⁽³⁴⁾. Nonetheless, the presence of a developing tissue at the apical end of a growing root makes it an appealing object of further research to better understand the role played by this tissue in root development and how it can be used to our advantage for promoting root elongation and closure for necrotic immature permanent teeth, while pushing towards a more controllable and regenerative outcome. Consequently, it is paramount to develop an experimental model for studying the regenerative capacity of the apical papilla tissue.

1.5 Why scaffold-free tissue engineering?

Scaffold-free tissue engineering (SFTE) is a fast-growing subdiscipline of tissue engineering that has appealed to multiple researchers across different fields. Perhaps the most obvious advantage over conventional scaffold-based engineering techniques –as suggested by the name– is that SFTE waives off the need for using an exogenous scaffold, thereby evading most of the challenges secondary to scaffold use, such as the immunologic response to the scaffold material, the inhomogeneous cell distribution and the low cell survival due to limited nutrient intake⁽³⁵⁻³⁷⁾. On a different note, scaffold-free techniques reinforce the cells' innate ability to deposit extracellular matrix, thereby paving the way for more direct mechanotransduction and enhanced tissue integration⁽³⁸⁾. To date, SFTE has been used with multiple cell sources for various regenerative purposes, including myocardial patches⁽³⁹⁾, arterial grafts⁽⁴⁰⁾, corneal grafts⁽⁴¹⁾,

pancreatic islet cell sheet grafts⁽⁴²⁾, oral mucosal cell sheet grafts for oesophageal ulceration⁽⁴³⁾, dermal fibroblast sheet grafts for pleural defects⁽⁴⁴⁾ and periodontal ligament cell sheets for periodontal regeneration⁽⁴⁵⁾. Scaffold-free engineering techniques mainly encompass both 2D and 3D cultures. In addition to the assets offered by SFTE, a 3D scaffold-free culture offers the leverage of having more cell junctions, which allows for better cell-cell communication and a more accurate emulation of the tissue response to mechanical stimuli. Moreover, 3D cultures generate gene and protein expression profiles that more closely resemble those of their innate tissue counterparts than 2D cultures⁽⁴⁶⁾.

The advantages offered by this technique make it quite suitable for generating models to study normal development, as well as disease conditions. As a developmental model, SFTE grants the cells autonomy to self-organize, recreating the architectures seen in developing tissues in vitro⁽⁴⁷⁾. This allows for a comparably more faithful simulation of the conditions of normal development, when compared to the use of a synthetic scaffold. As such, scaffold-free organoids have emerged as 3D self-organizing models for studying disease and development. Organoids are basically 3D in-vitro cultures that self-organize into constructs that mimic their corresponding in-vivo organ⁽⁴⁸⁾. Examples of oral organoids are salivary gland organoids from embryonic stem cells^(49, 50), tooth germ organoids from dissociated dental epithelial and dental mesenchymal cells^(51, 52), tooth germ-like organoids from induced pluripotent stem cells with dental epithelial or mesenchymal cells^(53, 54) as well as a tooth germ organoid from dental pulp cells and epithelial cells⁽⁵⁵⁾.

Our research group has also developed dental organoids utilizing different types of dental stem cells. The technique of scaffold-free tissue engineering predominately used by our group involves isolating human dental stem cells from extracted third molars and culturing the cells in

an osteogenic medium to form a cell sheet which, when robust enough, is detached from the substratum and finally contracts into a 3D construct toward two pins that are placed 4-7 mm apart, to form a cylindrical-shaped construct that is comprised solely of the cells and their endogenous matrix. Our group has shown that constructs of dental-pulp-derived cells organized into a dentin/pulp-like organoid⁽⁵⁶⁾, whereas constructs of periodontal-ligament-derived cells organized into a cementum/PDL-like complex⁽⁵⁷⁾. Consequently, it would be worthwhile to investigate the self-organization potential of scaffold-free engineered apical papilla cells, in an attempt to better understand their regenerative potential.

There are several factors, however, that can influence tissue organization and patterning. Some of these factors are mode of perfusion of the tissue in culture, mechanical properties of the substrate, mechanical forces applied during culture and the final size of the organizing tissue^(58, 59). Force sensing and geometry sensing have also been described as factors regulating cell functions⁽⁶⁰⁾. Therefore, our study employed scaffold-free tissue engineering to create dental organoids from SCAP to observe their ability to self-organize in vitro and to note differences in the final tissue pattern in response to variation in the type of substrate used and the final geometry of the organoid.

2.0 HYPOTHESIS

Objective: The objective of our study was to engineer scaffold-free dental organoids using stem cells from the apical papilla (SCAP), as a 3D experimental model for studying the regenerative potential of SCAP.

Hypothesis: Our hypothesis is that the scaffold-free dental organoids engineered using SCAP will self-organize into a spatially organized dentin/pulp-like complex.

Specific aim of the study: Engineer and histologically characterize the scaffold-free SCAP organoids generated on different substrates and with different final organoid shapes after in vitro culture.

3.0 MATERIALS AND METHODS

3.1 Apical papilla cell isolation, expansion and storage

The apical papilla tissue was isolated from the immature roots of adult human 3rd molars that had been collected from the Oral and Maxillofacial Surgery Clinic at University of Pittsburgh, School of Dental Medicine. All teeth used for this study were free from caries or infection. They were collected and transferred to our lab in a solution of phosphate buffer saline (PBS) with penicillin and streptomycin (pen/strep; Gibco Life technologies corporation, USA) (PBS+2X pen/strep) within 24 hours of their extraction. The apical papilla tissue was trimmed off the root end using tweezers and scalpel, and then transferred to a conical tube containing Dulbecco's Modified Eagle Medium (DMEM; Gibco Life technologies corporation, USA), 20% fetal bovine serum (FBS; Atlanta biological, USA) and 1% pen/strep. The isolated apical papilla tissue was minced on the following day using the blades of two orthogonally positioned scalpels. First, it was transferred to a petri dish containing 2-3 ml of DMEM and the scalpel blades were used to cut the tissue into $\sim 1\text{mm}^2$ pieces. The minced tissue was then collected into a conical tube containing DMEM and centrifuged for 5 minutes at 2000 rpm to form a pellet. The medium was poured off and the pellet was resuspended in 2ml of digestion cocktail of collagenase (3mg/ml) and dispase (4mg/ml) (Worthington biochemical, USA). It was placed in a 37°C water bath for ~ 30 minutes, with agitating the tube every 10 minutes, until the digested tissue suspension turned opaque denoting proper digestion of the tissue. The digested tissue suspension was then passed through a $70\mu\text{m}^2$ cell strainer to obtain a single-cell suspension. The cells were then cultured in a T75 flask containing regular growth medium (henceforth referred to as M0). M0 is made of DMEM, 20% FBS and 1% pen/strep.

Once the cells reached ~80% confluence, the growth medium was aspirated from the flask, the adherent cells were then washed with sterile PBS(Corning, USA) and trypsinized by incubating them in 2ml of 0.05% of trypsin-EDTA (TrypLE™ Express;Gibco Life technologies corporation, USA) at 37°C for 3-5 minutes, until the cells were detached from the flask base and were freely floating in the flask (as observed under light microscope). The trypsin was then deactivated by adding in 8ml of M0 and a cell count was done with trypan blue stain (Gibco Life technologies corporation, USA) using a hemocytometer, where the trypan-blue-stained dead cells were excluded from the count. The cell solution was centrifuged and resuspended in freeze medium [made of 10% dimethyl sulfoxide “DMSO” (Sigma-Aldrich, USA) in M0] and then aliquoted in cryovials, each containing 1ml of cell solution at a concentration of $\sim 1 \times 10^6$ cells/ml for cryogenic storage in liquid nitrogen at -196°C for future use. For our experiments, cells between passage 3-5 were used.

3.2 Confirmation of osteogenic potential of the isolated SCAP

For osteogenic differentiation, the cells were first plated in M0 and the medium was switched to an osteogenic medium 48 hours after plating. This was made of DMEM (Gibco Life technologies corporation, USA), 20% fetal bovine serum (Atlanta biological, USA), 1% penicillin & streptomycin (Gibco Life technologies corporation, USA), 5mM β -GP (Acros/Fisher, USA), 50 μ g/ml ascorbic acid (Fisher Chemical, China) and 10nM dexamethasone (Sigma-Aldrich, USA). The medium was changed every 48-72 hours and the cells were cultured for approximately 3 weeks. For the controls, the medium was never switched to osteogenic medium, and the cells remained in M0 for the entire 3 weeks

After ~3 weeks, the medium was aspirated and the cell sheets were washed 3 times with 1x PBS and then fixed in 4% paraformaldehyde for 15 minutes, followed by rinsing 3 times with 1x PBS

The PBS was then aspirated and ~1ml of 2% alizarin red S stain was dispensed into each well of the 6-well plate, enough to cover the whole cell layer. The stain was left for ~20-30 seconds and was aspirated once a color change was noticed in the cell layer. The staining fluid was then aspirated, and the plates were sealed and stored at -20°C until quantification.

For quantification, 2.5ml of solubilization solution (5% Sodium Dodecyl Sulfate + 1.8% HCl) were added in each well and the plates were incubated on a shaker at room temperature for 10 minutes. 150µL of the sample extracted from each well was transferred to a 96-well plate in triplicates (i.e. 450µL from the sample extracted from each well was transferred to fill 3 wells in the 96-well plate, with each well receiving 150 µL). A standard curve was created using the prepared solubilization solution + Alizarin Red S stain, creating a gradient concentration (500µg/mL, 250µg/mL, 125µg/mL, 50µg/mL, 25µg/mL and 12.5µg/mL). Optical density of the samples was measured via microplate reader (Biotek Synergy™ Microplate Reader H1) at OD 405nm and the total Alizarin Red S stain present in the sample was calculated relative to the standard curve using the software GEN5 (version 2.07). A two-sample t-test was performed to determine the p-value. A p-value of <0.05 was considered statistically significant.

3.3 Engineering of the 3D organoids

For our experiments, we had 3 experimental conditions; plating the cells on laminin-coated polydimethylsiloxane-coated plates (henceforth referred to as PDMS/laminin-coated plates) and plating the cells directly on tissue culture plastic (TCP). The PDMS/laminin-coated group had two conditions for engineering the constructs; the first was without the use of pins, and the second was with the use of pins (will be further described).

For the PDMS/laminin-coated group, PDMS (SLYGARDTM™, USA) was prepared by adding the base to the curing agent in a ratio of 9:1 and then stirring the mix in a plastic beaker using a plastic spatula. Then, 2ml of the PDMS mix was used to coat each well in the 6-well plate using a 10ml syringe. The plates were left to dry in the fume hood overnight and were then left for an additional 24 hours with the plate lid on.

To facilitate cell adhesion on the PDMS-coated plates, the PDMS was coated with laminin. First, the PDMS-coated plates were washed once with 70% alcohol and twice with sterile PBS (Corning, USA). Then, the laminin coating was prepared by adding laminin (Gibco, USA) to sterile PBS at a concentration of 9.62µg/ml. Lastly, 3ml of the laminin solution were dispensed in each well and the plates were left to dry overnight in a sterile hood. On the next day, sterile PBS was used to rinse the PDMS/laminin-coated plates twice and the plates were further sterilized by incubating them for one hour under UV light in the sterile hood. After that, ~1ml of M0 was added to each well and the 6-well plates were left for least 24-48 hours in the incubator (at 37°C, 5% CO₂) before proceeding with cell plating, as this has been noted to enhance cell adhesion.

The cells were plated in M0 in 6-well plates with 2ml in each well at a cell density of 100,000 cells/ml. The medium was changed every 48-72 hours. On the first media change, the medium was switched to osteogenic medium (M1) containing DMEM (Gibco Life technologies corporation, USA), 20% FBS (Atlanta biological, USA), 1% pen/strep (Gibco Life technologies corporation, USA), 5mM beta-glycerophosphate (β-GP; Acros/Fisher, USA), 50µg/ml ascorbic acid (Fisher Chemical, China), 10nM dexamethasone (Sigma-Aldrich, USA), 5ng/ml FGF-2 (Peprotech, USA).

On the next media change, the medium was changed to a low-serum osteogenic medium (henceforth referred to as M2) made of DMEM (Gibco Life technologies corporation, USA), 5% FBS (Atlanta biological, USA), 1% pen/strep (Gibco Life technologies corporation, USA), 5mM β-GP

(Acros/Fisher, USA), 50 μ g/ml ascorbic acid, 10nM dexamethasone , 5ng/ml FGF-2 and 2ng/ml TGF- β 1 (Peprotech, USA).

The cells were kept in culture, with changing the medium every 2-3 days. After the first 2-3 days of being in M2, it was observed that the cell sheet was starting to detach itself from the underlying substrate, starting out at the edges of the well (as observed under the microscope). For the PDMS/laminin-coated group, the cell sheet usually detached itself fully from the substrate without the need for any assistance. For the tissue culture plastic (TCP) group, however, the cell sheet required further assistance to fully detach from the plastic substrate. This was done with the help of a sterile pipette tip that was used to aid in gently detaching the cell sheet from the underlying substrate. The floating cell sheet would take about 2-3 additional days to self-contract into a 3-dimensional ball-like tissue construct. For the PDMS/laminin-coated group, we had two sub-groups of experimental conditions. In the first, we let the cell sheet detach itself from the substrate and contract on its own into a ball-shaped 3-dimensional tissue construct. The second condition utilized sterile 0.2mm-thick stainless-steel pins, where two pins were placed 4mm apart in each well (on the same day of changing to M2) and the pins were anchored into the soft PDMS substrate. This allowed the cell sheet to contract toward the 2 pins, forming a cylindrical-shaped tissue construct. The 3D constructs in the three experimental conditions were then left in culture for 1 or 2 weeks, after which the tissue constructs were fixed for characterization.

A total of ~120 constructs were engineered. They were subdivided into 3 experimental groups: TCP group (n = 62), PDMS/laminin+pins group (n = 26) and PDMS/laminin-pins (n = 32)

3.4 Histological characterization of the engineered 3D SCAP constructs

The engineered SCAP constructs were washed twice with PBS and then fixed with 10% formalin at 4°C overnight. On the next day, the constructs were rinsed in PBS and stored in 70% ethanol at 4°C for at least 24 hours before being processed. (Note: A few drops of Eosin stain were added to the 70% alcohol to allow the constructs to minimally take up the pink stain, for easier identification of the samples during paraffin embedding). The constructs were processed in a tissue processor (LEICA ASP300S, Leica Instruments GmbH Germany) for paraffin embedding. A microtome (LEICA RM2135 style, Leica Instruments GmbH Germany) was used to cut five-micrometer-thick tissue sections from the paraffin-embedded tissue samples and the sections were mounted on glass slides. The tissue sections were then deparaffinized and rehydrated through a series of washes in xylene (2X 5 minutes each), 100% ethanol (2X, for 5 and 2 minutes respectively), 95% ethanol (2X, 2 minutes each) and lastly distilled water. The rehydrated tissue sections were now ready for further processing to be stained with Hematoxylin and Eosin (H&E), Alizarin Red S (AR) and immunostaining.

3.4.1 Hematoxylin and Eosin stain

The rehydrated tissue sections were stained with Hematoxylin and Eosin stain “H&E” (Richard-Allan scientific, Thermo Scientific, USA) through a series of washes in: Hematoxylin (2-minute incubation), Water (20 rinses), Acid/alcohol “Nu-clear” (3 rinses), Bluing reagent “Scott’s tap water substitute” (30-second incubation), Water (20 rinses), 70% ethanol (1 rinse), Eosin (40-second incubation), 95% ethanol (2X, 15 rinses each), 100% ethanol (2X, 15 rinses each) and lastly xylene (2X, 15 rinses each). The slides were then mounted with a xylene-based mounting medium (Cytoseal™

60, Thermo Scientific, USA) and lastly cover-slipped to be analyzed under the microscope. The microscopic images were captured using Nikon TE-2000.

3.4.2 Alizarin Red S stain

The Alizarin Red staining solution was prepared by dissolving 1gm of Alizarin Red S (Sigma-Aldrich, China) in 50ml of distilled water. The pH of the final solution was adjusted using ammonium hydroxide “NH₄OH” (diluted 1:100) to be within the range of 4.12-4.16. A PAP pen was used to create circular markings around the tissue sections on each glass slide, to create a hydrophobic barrier around each tissue section. Using a pipettor, the Alizarin Red stain was dispensed on each tissue section and left for a maximum of 30 seconds, or until an uptake of the red color was observed (whichever comes first). Excess Alizarin Red was then dabbed off the slide and the slide would then be rinsed through a series of washes in acetone (10 rinses), acetone/xylene “1:1” (10 rinses) and lastly xylene (10 rinses). The slides were then mounted with a xylene-based mounting medium (Cytoseal™ 60, Thermo Scientific, USA) and cover-slipped. The microscopic images were captured using Nikon TE-2000.

3.4.3 Immunostaining

Heat-induced epitope retrieval: The tissue sections were incubated overnight in a 10mM Citrate +0.05% Triton X solution (Sigma-Aldrich, USA) at 60°C overnight. They were then rinsed twice with cold water.

Permeabilization and Blocking: The tissue sections were first permeabilized in 0.1% triton X (Sigma-Aldrich, USA) in PBS for 10 minutes. The slides were then rinsed with PBS (3X, 5 minutes each). After rinsing, excess PBS was dabbed off and the tissue sections on each slide were separated by circular markings around each section using PAP pen. Using a pipettor, blocking solution was

dispensed onto each tissue section. The blocking solution was prepared using 5% goat serum (MP Biomedical, LLC, USA) and 0.05% Tween 20 (Sigma-Aldrich, USA) in PBS. The tissue sections were incubated with the blocking solution for 1 hour at room temperature, for the purpose of minimizing unspecific binding of the primary antibody.

Primary Antibodies: After the blocking step, primary antibody in blocking solution or blocking solution only (for negative controls) was dispensed onto each tissue section. A list of the primary antibodies used in these experiments and their respective dilutions can be found in Table 1. The tissue sections were incubated overnight at 4°C.

Table 1 Primary antibodies

Primary antibody	Brand	Dilution
Dentin sialoprotein (DSP) antibody	Abcam catalog# ab216892	1:25
Dentin matrix protein 1 (DMP-1) antibody	Kerafast, Inc.© LF-148	1:100
Asporin antibody	Abcam, catalog# ab58741	1:100

Secondary Antibodies: On the next day, the tissue sections were rinsed (3X, for 5 minutes each) with PBS-T (0.05% Tween 20 in PBS). This was done by adding the PBS-T on each tissue section, using a pipettor, and then placing the slides on a shaker (at ~60-70 rpm) for 5 minutes for proper agitation of the rinse. (Note: the PAP pen markings around each tissue section keeps the PBS confined to each tissue section). This was repeated thrice, by using a suctioning unit to gently suction away the old PBS-T rinse in between the rinses. The sections were now ready for incubation in the secondary antibody, where secondary antibody in blocking solution was dispensed onto each tissue section and incubated for one hour at room temperature. The type and dilution of the used secondary antibody is found in table 2.

Table 2 Secondary antibody

Secondary antibody	Brand	Dilution
Alexa Fluor™ 488	Invitrogen, ThermoFischer, USA	1:500

DAPI counterstaining and Mounting: By the end of the incubation period, the sections were rinsed with PBS (3X times, 5 minutes each). (Note: the same technique of rinsing that was explained above was used here). The sections were counterstained with 4',6-diamidino-2-phenylindole “DAPI” (Sigma-Aldrich, USA) to stain the nuclei. This was done by adding DAPI in PBS (1:250) onto each tissue section (with the use of a pipettor) and incubating the slides for 5 minutes. The slides were again rinsed with PBS (3X times, 5 minutes each, using the same technique). Finally the slides were dipped quickly in distilled water, dabbing off the excess after, and then mounted with aqueous mounting media (Shandon Immu-Mount™, Thermo Scientific, USA) and coverslipped.

The microscopic images were captured using Nikon ECLIPSE Ti microscope and processed in NIS Elements Viewer software.

3.5 Fourier-transform infrared spectroscopy (FTIR)

The organoids were rinsed using distilled water, followed by flash freezing them in liquid nitrogen. The samples were lyophilized in the tissue lyophilizer overnight and then stored at -20 °C until they were analyzed by FTIR spectrometer. The samples were analyzed by collecting 128 scans at a resolution of 4 cm⁻¹ using Bruker Vertex 70 spectrometer (Billerica, MA). The data were presented using OriginPro software, courtesy of Prof. Elia Beniash.

4.0 RESULTS

4.1 Morphology and osteogenic differentiation capacity of SCAP

We isolated SCAP from extracted 3rd molars and observed the cells under light microscope the next day of plating, to assess their morphology. It was noticed that the cells assumed a spindle-shaped morphology which is commonly seen with mesenchymal stem cells (Fig.4A, A'). To confirm the osteogenic potential of the isolated cells, the cells were cultured in an osteogenic medium for approximately 3 weeks. The results revealed abundant deposition of calcium demonstrated by the heavy Alizarin red S stain, which was significantly greater than the much lighter stain in the control samples (Fig.4B, C) with a p-value of 0.00078.

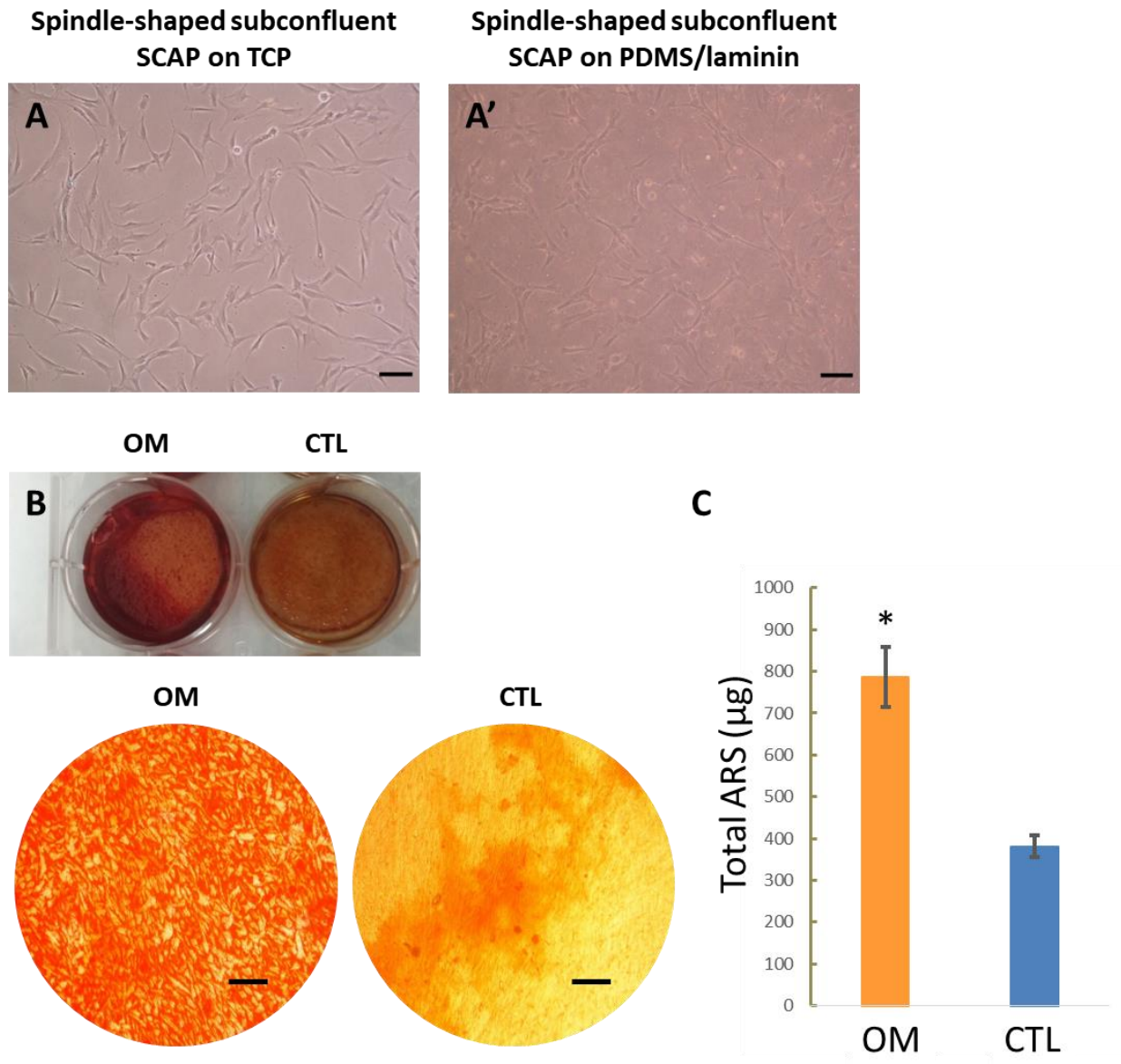


Figure 4 Isolation, culture and osteogenic differentiation of SCAP. (A): Phase contrast micrograph showing spindle-shaped morphology of SCAP {Scale bar = 100µm}; (B): Alizarin Red S staining after osteogenic induction of SCAP; (C): Quantification of alizarin red S stain in micrograms ($p < 0.01$). {CTL: Controls that received growth medium, OM: Osteogenic medium; Scale bar = 100µm}

4.2 Generating the 3D SCAP organoids

The experimental design included culturing SCAP under 3 experimental conditions: directly onto tissue culture plastic (TCP), on PDMS/laminin substrates with stainless-steel pins (PDMS/laminin+pins), and on PDMS/laminin substrates without the stainless-steel pins (PDMS/laminin-pins) After cell sheet formation and contraction, a 3-dimensional tissue construct was formed. The constructs were allowed to sit in osteogenic medium for 1 or 2 weeks post-formation, after which they were fixed for characterization. A schematic of the experimental design can be seen in Fig.5.

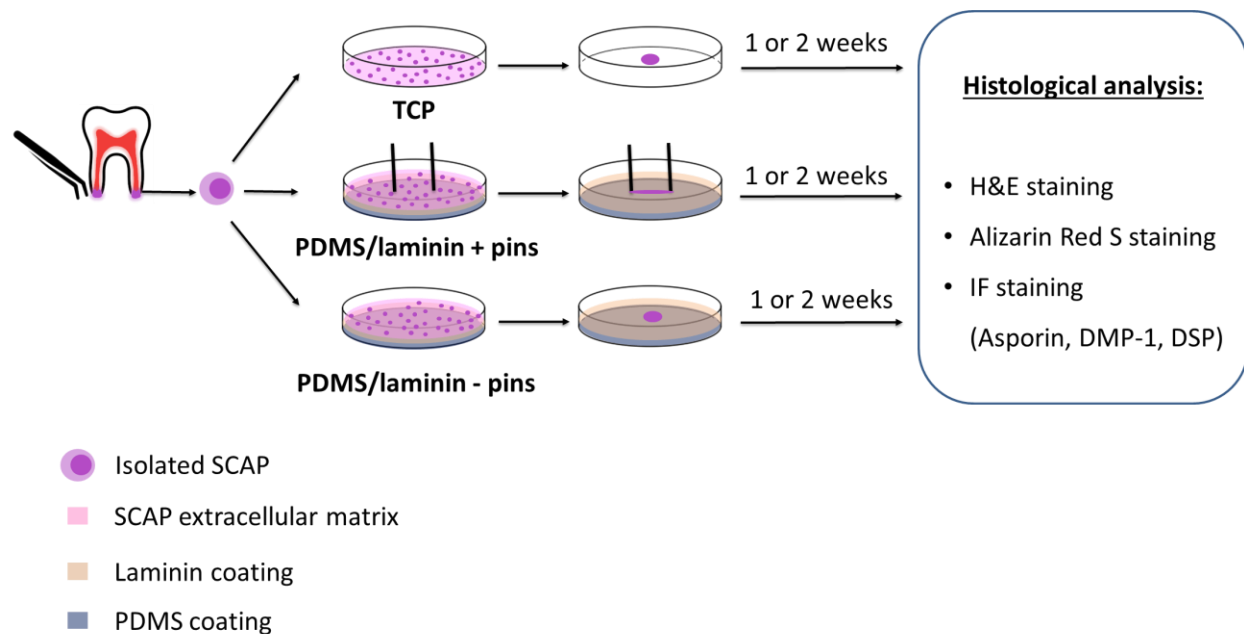


Figure 5 Experimental design of the study

The 3D SCAP organoids were successfully generated. For the ones cultured on tissue culture plastic (TCP), the cells reached confluence within 2-4 days of plating (Fig.6A) at a seeding density of ~200,000 cells/well in a 6-well plate and the resulting cell sheet started contracting off

the TCP starting out at the edges around day 6 of plating (Fig.6B). However, the cell sheet did not readily detach from the substrate and required gentle assistance with a sterile plastic pipette tip to fully detach (Fig.6C) and finally it tightened into a 3D ball-like tissue (Fig.6D). Similarly, for the ones cultured on the PDMS/laminin substrate, the cells reached confluence within 2-4 days of plating at the same seeding density in a 6-well plate (Fig.6A'), and the formed cell sheet contracted around day 4 of plating, leading to its full detachment from the underlying substrate at around day 6 (Fig.6B', C') and it finally tightened into a 3D tissue. For the group without the pins, the cell sheet freely contracted and rolled up into a ball-like tissue; whereas for the group where stainless steel pins were introduced into the system, the cell sheet was anchored on either end to one of the pins and as a result, contracted into a cylindrical-shaped tissue (Fig.6D').

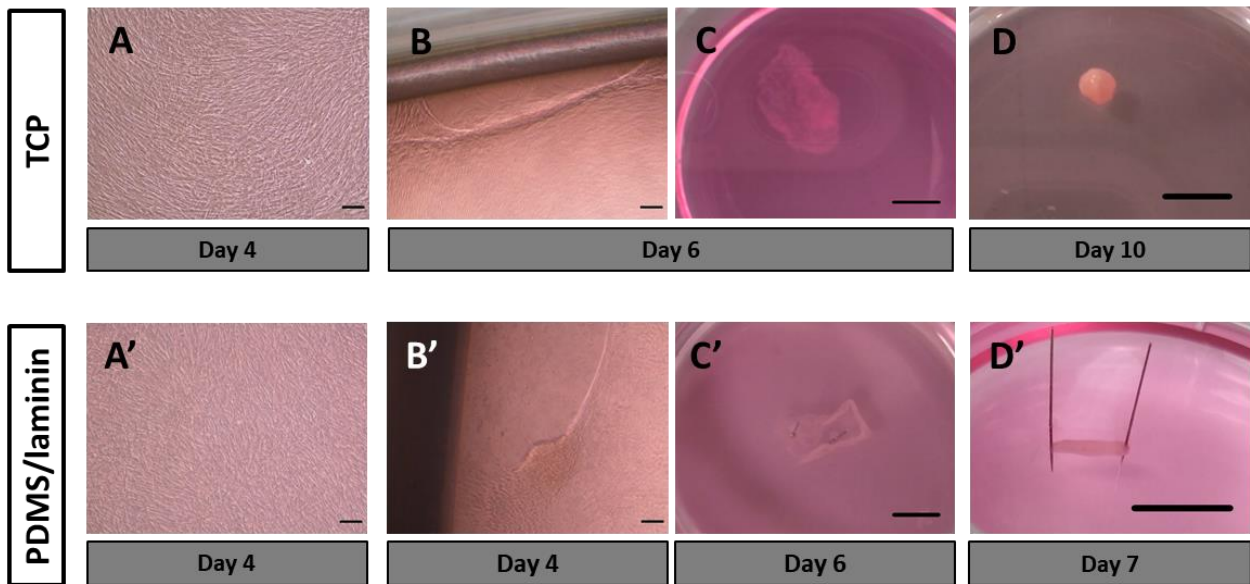


Figure 6 Engineering the dental organoids from SCAP.(A,A'): Confluent SCAP, (B,B'): The cell sheet as it detaches from the substrate starting at the edges, (C,C'): The cell sheet after either being gently assisted with detaching off the substrate (for the TCP group) or after spontaneously contracting off the substrate at day (for PDMS/laminin group), (D,D'): The engineered dental organoid after the SCAP cell sheet fully contracts into a 3D tissue construct. {TCP: Tissue Culture Plastic; PDMS/laminin: the laminin-coated, PDMS-coated substrates; Scale bar for (A, A', B, B') = 100 μ m; Scale bar for (C, C', D, D') = 5mm}

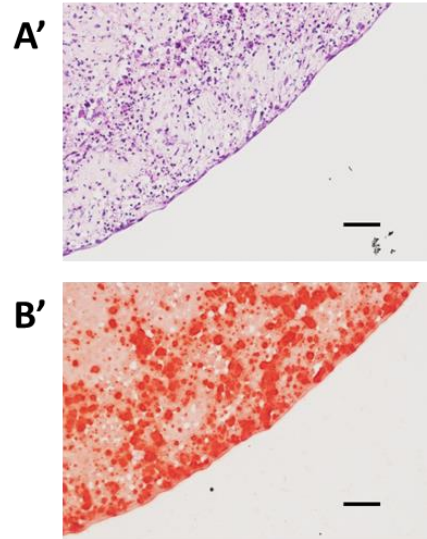
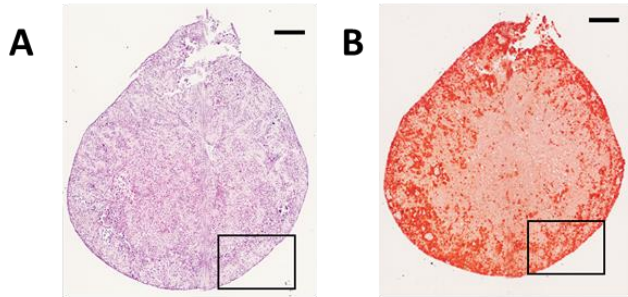
4.3 Histological evaluation of tissue morphology and mineral deposition in the SCAP constructs

Generally, the organoids in the three groups were cellular throughout their entire thickness. The organoids cultured on PDMS/laminin substrates were remarkably more densely cellular compared to the ones cultured on TCP.

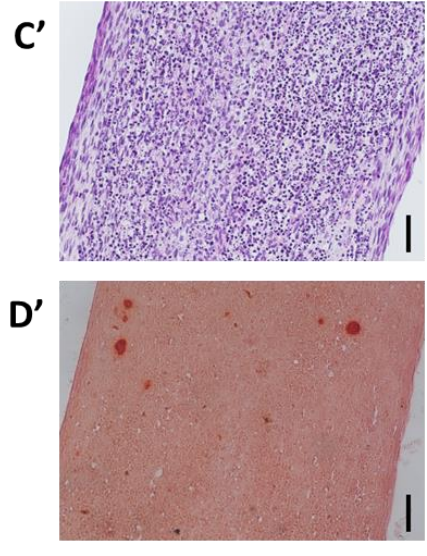
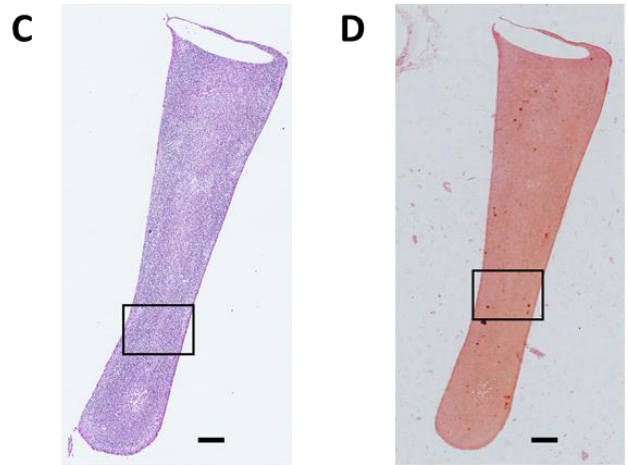
Low magnification H&E images of the SCAP organoids formed on TCP at the 1-week timepoint showed that the cells were loosely arranged within an abundant ECM network (Fig.7A). Higher magnification images showed generally rounded nuclei, with only one layer of seemingly flat nuclei at the border of the construct (Fig.7A'), possibly a result of the cells orienting differently to form the final layer that encircles the 3D organoid. Low magnification images of ARS staining revealed mineralization at the periphery of the construct, whereas the inner portion of the construct was unmineralized (Fig.7B). Higher magnification images revealed that the border of the 3D tissue was indeed mineralized, where the ARS included the outermost part of the organoid (Fig.7B').

For the organoids in the PDMS/laminin+pins group, low magnification H&E images at the 1-week timepoint showed that these organoids were densely cellular, with a high cell-to-ECM ratio (compared to the organoids from the TCP group) (Fig.7C). Higher magnification images revealed two distinct cell morphologies within the organoid: rounded cells along the bulk of the construct, and flat elongated cells along the periphery (Fig.7C'). With regard to ARS staining, the organoids in this group showed little-to-no mineralization, with only a few ARS-positive speckles (Fig.7D, D').

(i) TCP group



(ii) PDMS/laminin+pins group



(iii) PDMS/laminin-pins group

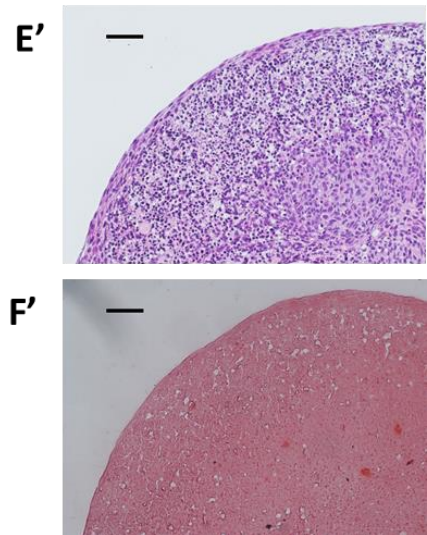
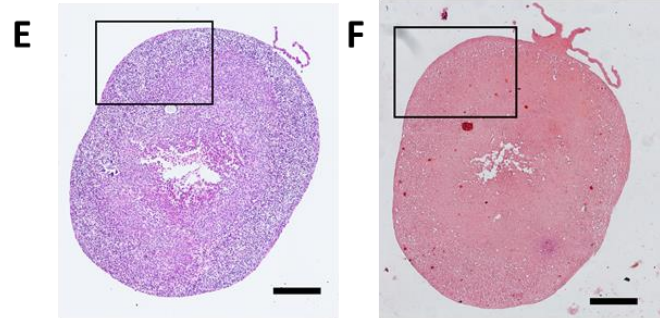
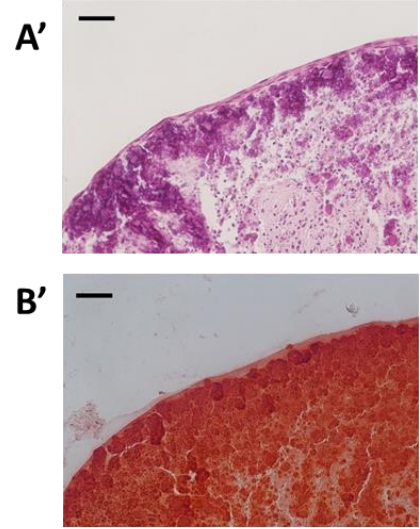
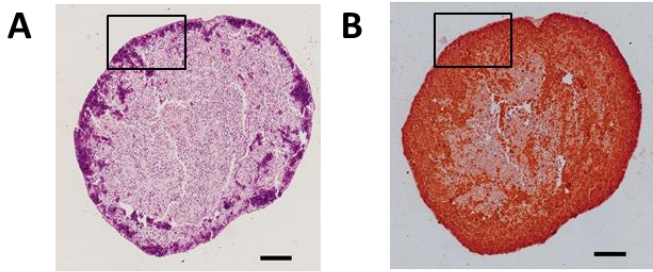


Figure 7 Histological analysis of SCAP organoids at one week (A, A’): H&E stain at low and high magnifications of a SCAP organoid from the TCP group at one week, & (B, B’): ARS stain at low and high magnifications of a SCAP organoid from the TCP group at one week. (C, C’): H&E stain at low and high magnifications of a SCAP organoid from the laminin (+) pins group at one week, & (D, D’): ARS stain at low and high magnifications of a SCAP organoid from the laminin (+) pins group at one week. (E, E’): H&E stain at low and high magnifications of a SCAP organoid from the laminin (-) pins group at one week, & (F, F’): ARS stain at low and high magnifications of a SCAP organoid from the laminin (-) pins group at one week. {Scale bar for low and high magnification images = 200µm & 50µm respectively }

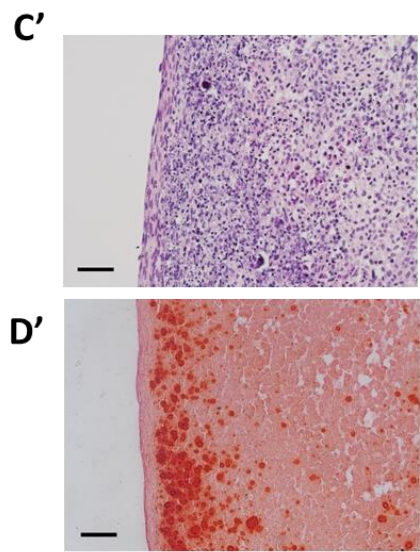
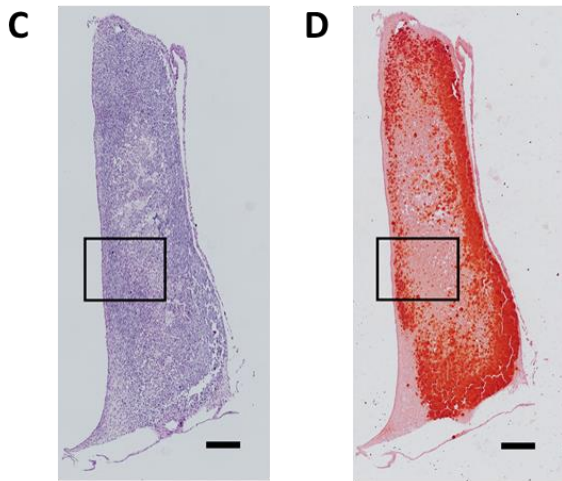
Low magnification H&E images of the SCAP organoids from the PDMS/laminin-pins group at the 1-week timepoint showed that these organoids were rounded in shape and were densely cellular (Fig.7E). Higher magnification images revealed a layer of elongated cells along the periphery of the organoid (Fig.7E’); however, this layer was not as accentuated as that seen in the pinned constructs. ARS staining showed little-to-no mineralization, with only a few ARS-positive speckles (Fig.7F, F’).

At two weeks, SCAP organoids formed on TCP showed much heavier mineralization, compared to the one-week organoids. The mineralization pattern was still discernible with the organoids maintaining a relatively unmineralized core (Fig.8A, B). Higher magnification images showed one or two layers of seemingly flat nuclei at the border of the construct, with the mineralization almost extending to the outermost part of the organoid (Fig.8A’, B’).

(i) TCP group



(ii) PDMS/laminin+pins group



(iii) PDMS/laminin-pins group

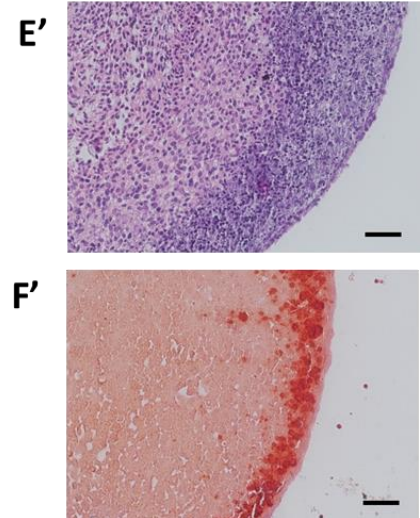
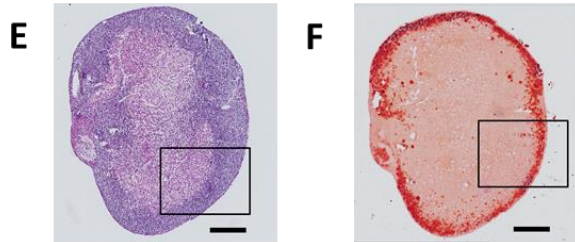


Figure 8 Histological analysis of SCAP organoids at two weeks (A, A’): H&E stain at low and high magnifications of a SCAP organoid from the TCP group at two weeks & (B, B’): ARS stain at low and high magnifications of a SCAP organoid from the TCP group at two weeks. (C, C’): H&E stain at low and high magnifications of a SCAP organoid from the laminin (+) pins group at two weeks & (D, D’): ARS stain at low and high magnifications of a SCAP organoid from the laminin (+) pins group at two weeks. (E, E’): H&E stain at low and high magnifications A SCAP organoid from the laminin (-) pins group at two weeks:& (F, F’): ARS stain at low and high magnifications of a SCAP organoid from the laminin (-) pins group at two weeks.. {Scale bar for low and high magnification images = 200µm & 50µm respectively }

Low magnification H&E images of the SCAP organoids from the PDMS/laminin+pins group at the 2-week timepoint showed that the organoids maintained their two distinct cell morphologies with their respective locations within the organoid: rounded cells along the bulk of the construct, flat elongated cells along the periphery (Fig.8C, C’). ARS staining at two weeks showed a peculiar mineralization pattern involving an outermost thin rim of unmineralized tissue (corresponding to the flat peripheral cells) that encloses a mineralized intermediate zone which exhibits a decreasing gradient of mineralization ending with an innermost core of unmineralized tissue (Fig.8D, D’), somewhat resembling the mineralization pattern seen in a tooth root, with outer unmineralized PDL, intermediate cemento-dentinal mineral and innermost unmineralized pulp.

Low magnification H&E images of the SCAP organoids from the PDMS/laminin-pins group at the 2-week timepoint showed that the organoids maintained their high cell density. Organoids in this group showed either only one layer of the flat elongated cells along their periphery, or this structure was lacking altogether (Fig.8E, E’). At two weeks, ARS staining was positive for this group. The organoids displayed a mineralization pattern close to that seen in the pinned groups, with (1) an unmineralized peripheral structure, (2) an intermediate mineralized

zone and (3) an innermost unmineralized central core, also similar to the organization that would be seen in a tooth root. Structures 2 and 3 were sharply delineated from each other in this group (Fig.8F, F'), as opposed to existing in the form of a gradient as seen in the pinned constructs.

4.4 Fourier-transform infrared spectroscopy (FTIR) analysis

FTIR was performed to further characterize the mineral within our organoids. The infrared spectrum (shown in Fig.9) showed an absorption band at 1000-1100 cm^{-1} denoting presence of phosphate, whereas the bands at 1600-1700 cm^{-1} and 1470-1570 cm^{-1} corresponding to amide I and amide II, respectively, denote presence of protein (possibly type I collagen).

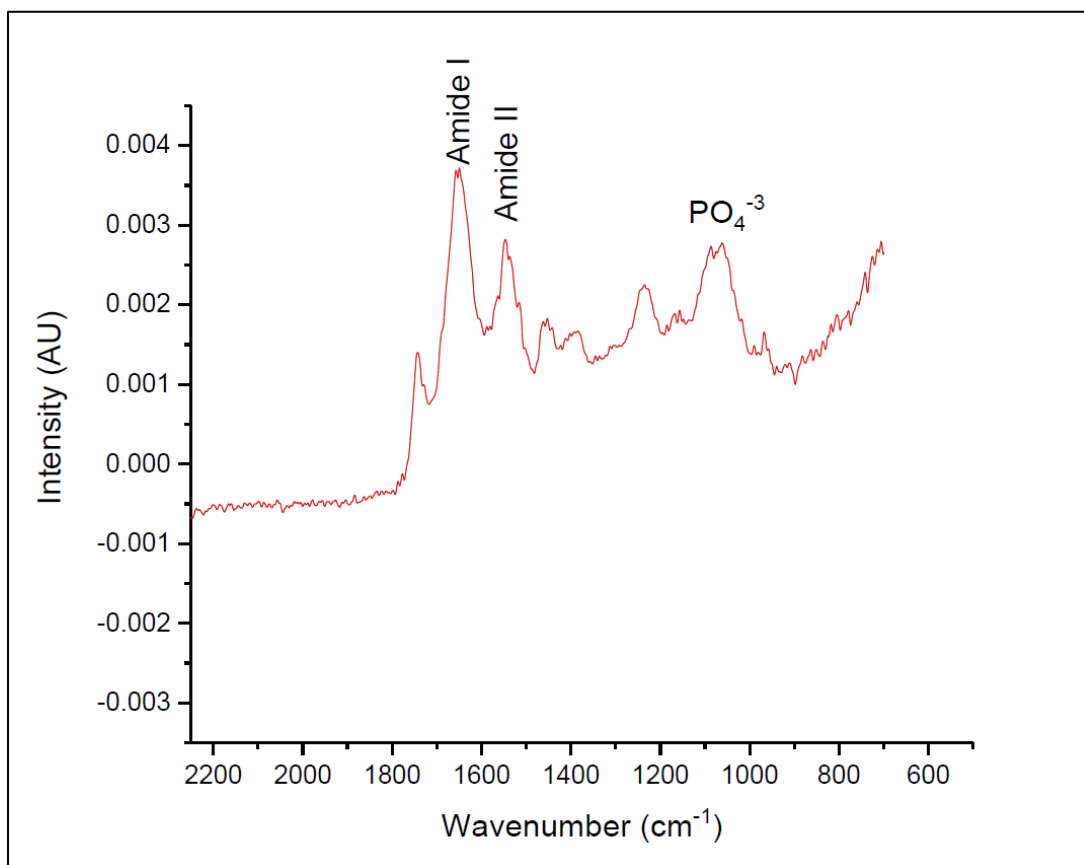


Figure 9 FTIR spectroscopy graph – Courtesy of Prof. Elia Beniash

4.5 Evaluation of protein expression in the SCAP constructs

Immunostaining was performed to detect localized protein expression in the SCAP constructs. Dentin sialoprotein and dentin matrix protein-1 were chosen, since these proteins are commonly used as odontogenic markers⁽⁶¹⁻⁶³⁾; whereas asporin –also known as periodontal ligament associated protein 1 (PLAP/1)– was chosen, since this protein has been reported as a periodontal ligament marker⁽⁶⁴⁾.

At one week, the pinned organoids in the PDMS/laminin+pins group showed diffuse positive expression of DSP, DMP-1 and asporin, denoting no specific tissue patterning at this timepoint with regard to protein expression (Fig.10).

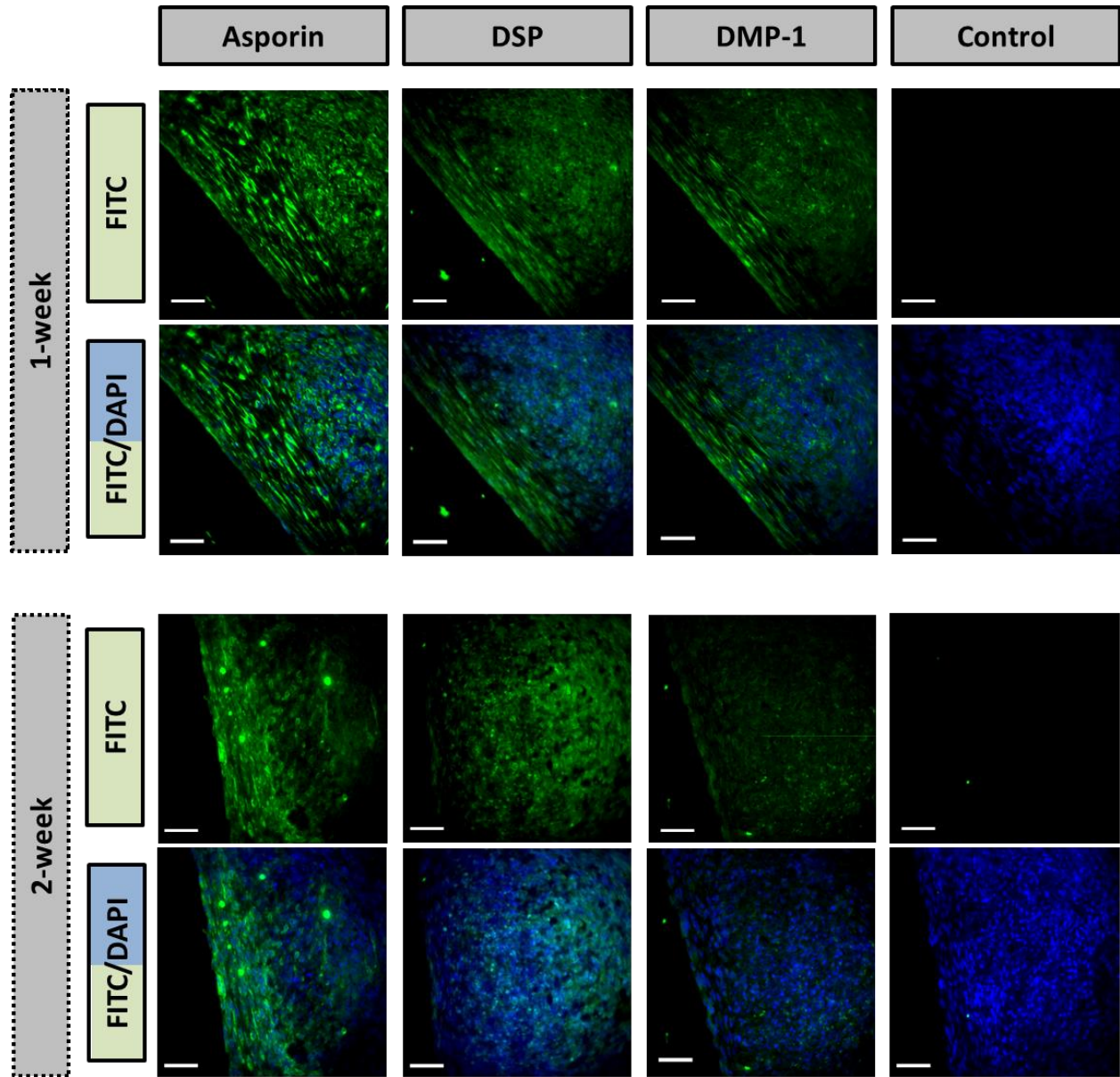


Figure 10 Protein expression analysis of SCAP organoids was performed to detect localization of DSP, DMP-1 and asporin expression. Proteins are shown in green; DAPI stain was used to detect nuclei (blue). {Scale bar = 50 μ m}

This, however, was only seen 50% of the time, whereas negative expression for DSP and DMP-1, with very minimal diffuse expression of asporin was seen in the other 50% (Appendix Fig.1), similarly suggesting no specific differentiation pattern.

At two weeks, the asporin expression became more localized to the peripheral part of the organoid, with reduced expression in the center. In contrast, the DSP expression was reduced around the periphery, and was more pronounced in the inner bulk of the organoid. DMP-1 expression was noted to be weak, with relatively elevated expression in the inner part of the organoid. This was suggestive that there were two different natures to the tissues within the organoid: a periodontal ligament-like tissue on the periphery, and a dentin-like tissue in the bulk of the organoid.

5.0 DISCUSSION

In this study, we aimed to create an experimental model for studying the ability of human stem cells from the apical papilla to self-organize into a dental organoid using a scaffold-free tissue culturing technique. The total population of cells from the apical papilla tissue of extracted 3rd molars was used in this study, and the cells were allowed to grow into a cell sheet that finally contracted into a 3D organoid. Scaffold-free tissue engineering (SFTE) was chosen as a technique for creating these organoids due to the advantages it offers such as minimizing external factors introduced by exogenous scaffolds, allowing for better cell-cell communication and providing a relatively more faithful reproduction of cell behavior within a tissue in comparison to scaffold-based engineered tissue. However, SFTE is not without its limitations. A scaffold-less engineered tissue lacks the structural support offered by a carrier scaffold. This can be a significant impediment to clinical translation, especially if the engineered tissue belongs to a load-bearing area, as mismatch in the functional properties between the immature implant and the fully mature neighboring native tissue can result in failure of the implanted tissue if prematurely loaded⁽³⁸⁾. This, however, may not be a significant drawback if the engineered tissue is of the non-load-bearing type. However, as a general disadvantage, SFTE largely requires greater cell-seeding density to allow for a structurally robust tissue of implantable size⁽⁶⁵⁾. This can cast doubt on the feasibility of this approach, especially with the issue of limited cell sources. Nonetheless, SFTE remains an important engineering technique that offers unique advantages offered by none of the available engineering modalities and one that is particularly suitable for creating models to study development.

Previously our research group has shown that scaffold-free tissue engineering of tooth-derived mesenchymal stem cells allows for formation of multi-tissue 3D structures that have a spatial organization similar to that seen in the anatomic organ from which each corresponding cell population was isolated. Dental pulp stem/progenitor cells formed organoids that had a mineralized periphery and an unmineralized core, similar to the organization pattern seen in a dentin/pulp complex. In addition, the mineralized peripheral tissue of the formed organoid expressed dentinogenic markers (DSP, DMP-1), whereas the unmineralized core did not⁽⁵⁶⁾. Conversely, periodontal ligament stem/progenitor cells formed organoids that had a mineralized core with an unmineralized periphery that expressed periodontal ligament markers (asporin, periostin) similar to the organization of a cementum/PDL complex⁽⁵⁷⁾. Following the same train of thought, we decided to explore stem/progenitor cells from the apical papilla and to test their capacity to undergo self-organization and to assess the tissues that these cells give rise to, as an experimental model system that can aid in better understanding the role that the apical papilla tissue plays during root development.

The mineralization pattern, as seen in the alizarin red S stains, in the SCAP organoids that were cultured on PDMS/laminin substrates resembled the pattern seen in a tooth root, with an outer unmineralized peripheral tissue (resembling unmineralized PDL), an intermediate mineralized tissue (resembling cementum/dentin) and innermost unmineralized tissue (resembling pulp). This mineralization pattern was different from the pattern seen in organoids previously engineered by our lab using dental pulp cells (DPCs). DPC organoids in the PDMS/laminin-pins group did not show a peripheral unmineralized rim (Fig.11: B, B' – Courtesy of Kristi Rothermund). The DPC organoids in the PDMS/laminin+pins group were engineered with the help of Tia Calabrese in the

lab and similarly had mineralization that extended to the peripheral part of the organoid along most of the organoid's bulk (Fig.11: D, D').

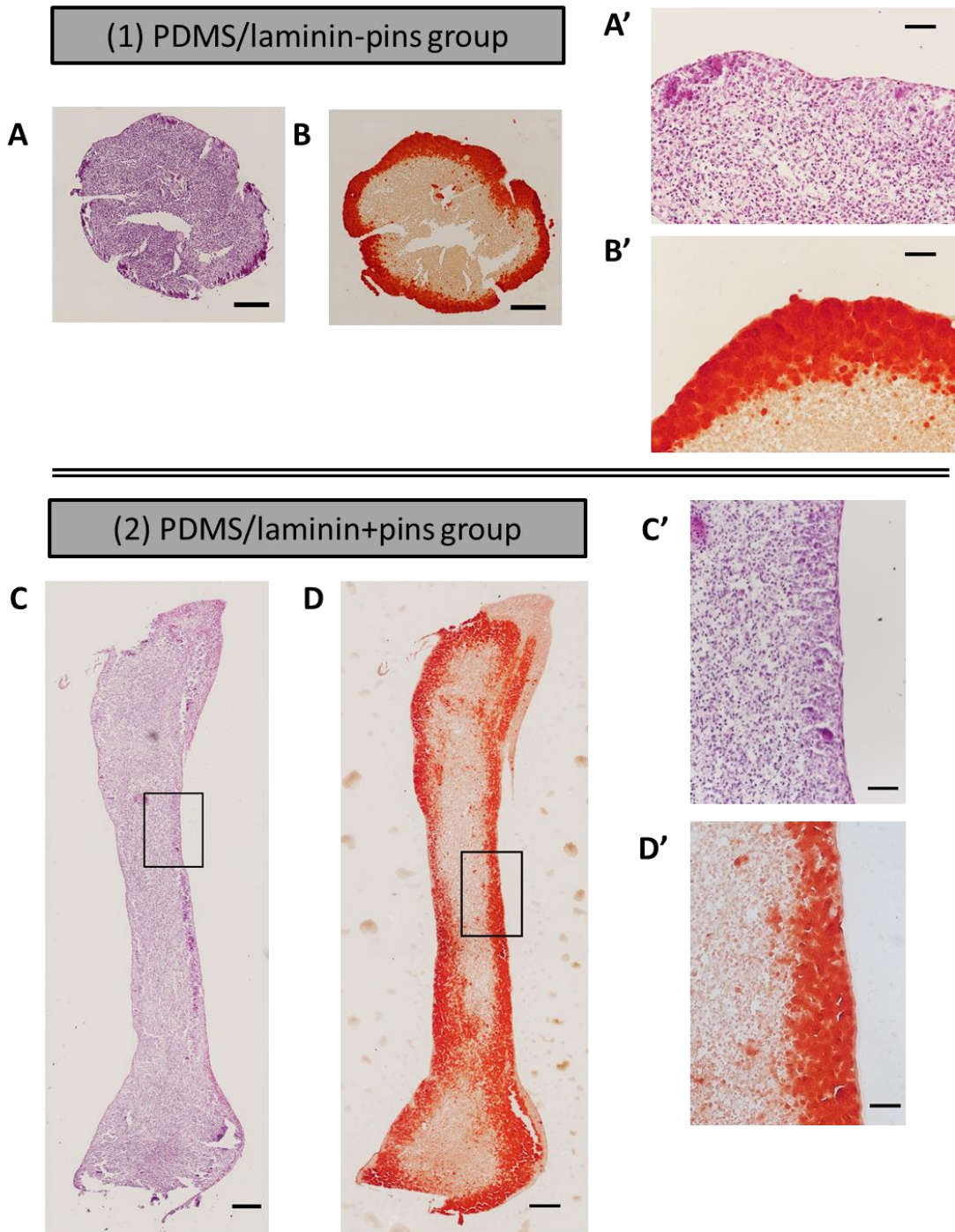


Figure 11 Histological analysis of DPC organoids (A, A'): H&E stain at low and high magnifications of a DPC organoid from the laminin (-) pins group at two weeks & (B, B'): ARS stain at low and high magnifications of

a DPC organoid from the laminin (-) pins group at two weeks. (Courtesy of Kristi Rothermund). (C, C'): H&E stain at low and high magnifications of a DPC organoid from the laminin (+) pins group at two weeks & (D, D'): ARS stain at low and high magnifications of a DPC organoid from the laminin (+) pins group at two weeks (Engineered by Tia Calabrese). {Scale bar for low and high magnification images = 200 μ m & 50 μ m respectively}

In our previous studies, the technique used involved culturing the cells on a PDMS/laminin-coated 6-well plate and later placing two stainless-steel pins to allow the cell sheet to contract toward them forming a cylindrical construct^(30,57). Here in the present study, we utilized the same technique (PDMS/laminin+pins); however, we performed two modifications to the system creating a total of 3 experimental conditions. The first modification was to exclude the use of the stainless-steel pins, allowing the cell sheet to freely contract into a 3D ball-shaped tissue. This condition was aimed at controlling for any effect introduced by the pins such as potential tensile forces they may be exerted on the cell sheet as it contracts and later, on the organoid as it further matures in vitro. The second modification was to culture the cells on tissue culture plastic substrates (without PDMS or laminin). This condition aimed at testing whether effects introduced by the substrate (such as the stiffness of the used substrate) would have an effect on tissue patterning. Interestingly, the results revealed a unique feature in the organization pattern in each of the three conditions, suggesting that not only were the pins affecting tissue patterning, but that the nature of the culture substrate was also contributing to the organization pattern seen in the final organoid.

At one week, the organoids that were formed on PDMS/laminin substrates were noted to generally have a thicker layer of distinctly more elongated cells on the peripheral border of the organoid, compared to the ones formed on TCP. This difference points to the probability that the

mechanical properties of the substrate can have an effect on the cells' cytoskeletal arrangement. This observation is in accordance with the study by Zhou et al.⁽⁶⁶⁾ where it was found that SCAP cultured on softer PDMS had a more spread-out morphology and an altered cytoskeleton compared to those cultured on stiffer PDMS. Similarly in our study, we saw a comparable difference between SCAP cultured on PDMS (the softer substrate) and on TCP (the stiffer substrate). Interestingly, the peripheral elongated cell layer almost disappeared in the PDMS/laminin-pins group at two weeks. This could be owed to the fact that at two weeks, the 3D organoid was now fully mature and freely floating in the culture-well and was no longer in contact with the underlying substrate. As a consequence, the integrin receptors of the cells at this point would have lost any mechanochemical cues they may have been receiving from the underlying substrate at an earlier timepoint. The same observation, however, was not seen in the PDMS/laminin+pins group at two weeks. This could potentially be because in the PDMS/laminin+pins group, the overall shape of the final organoid was changed (from a rounded to a cylindrical form) probably secondary to potential mechanical forces exerted by the pins. This introduced another variable which can influence cell morphology. Indeed, it was noted that whether at one or two weeks, the organoids in the pinned group had a significantly thicker peripheral layer of flattened cells than that seen in the other two groups. This can be attributed to the pins exerting some form of tensile force on the cells, thereby affecting their morphological differentiation. A study by Virjula et al.⁽⁶⁷⁾ noted something similar with human adipose stem cells cultured under cyclic equiaxial stretching. The study observed that the stretched cells exhibited smaller cell bodies and generally had a "star-shaped morphology".

Similar to cell morphology, the mineralization pattern seen within our final organoids also differed according to the culture conditions. At one week, mineralization was observed in only the

TCP group, with little-to-no mineralization in the PDMS/laminin groups; suggestive of substrate mechanics playing a role in cell differentiation. It is almost well established now that stiffer substrates enhance osteogenic differentiation of mesenchymal stem cells with several reports including bone marrow stem cells^(68, 69), periodontal ligament stem cells⁽⁷⁰⁾ and dental pulp stem cells⁽⁷¹⁾. In addition, the same phenomenon was previously observed with stem cells from the apical papilla, where stiffer substrates were noted to enhance their expression of osteogenic and mineralization marker genes⁽⁷²⁾. As a result, it was not surprising to find that the organoids on the TCP substrates mineralized earlier than the ones on the PDMS/laminin substrates, since a stiffer substrate such as TCP would be expected to encourage the cells' early commitment toward an osteogenic lineage.

Organoids from the TCP group at one week, showed mineralization at the very border of the construct, leaving an unmineralized core. At two weeks, the mineralization was more extensive, growing more toward the center of the construct; however, the core of the organoid remained relatively unmineralized at its center. This suggests that the direction of mineralization starts out at the periphery of the construct and moves inwards as the organoid is left for a longer time in the osteogenic medium. Interestingly, the mineralization pattern for the two-week-old organoids from the PDMS/laminin groups was remarkably different from that seen in the TCP group. In both PDMS/laminin groups, the mineralization did not extend to the outermost layer of the organoid, but rather left a thin rim of unmineralized tissue. This layer seemed to correspond to the peripheral tissue layer with the more elongated cell morphology seen in the pinned group. The nature of this peripheral tissue was intriguing, and therefore immunofluorescent protein tagging was performed for the PDMS/laminin+pins group specifically, considering that this unmineralized peripheral tissue was thickest and most consistent in this group, possibly owing

to the mechanical tension exerted by the pins, as previously alluded to. Another difference was noted in the interface between the mineralized intermediate portion and the unmineralized innermost core in the organoids that were pinned versus the ones that were not. In the PDMS/laminin-pins group, the interface between the two zones was more distinct, whereas in the PDMS/laminin+pins group, the mineral was in the form of a gradient of decreasing mineralization towards the center of the organoid with generally more mineral seen in the organoids where the pins were used, suggesting that not only were the pins causing morphological changes in the cells as previously mentioned, but they were potentially also having an effect on cell differentiation toward an osteogenic lineage. This has been reported with other mesenchymal stem cells such as periodontal ligament stem cells⁽⁷³⁾, bone marrow stem cells⁽⁷⁴⁾ and adipose stem cells⁽⁷⁵⁾, where tensile forces were noted to stimulate osteogenic cell differentiation and promote the expression of osteogenic genes.

Dentin sialoprotein (DSP) and dentin matrix protein-1 (DMP-1) are non-collagenous proteins expressed in dentin and bone ⁽⁷⁶⁻⁸¹⁾. DSP is released as a product of the proteolytic cleavage of dentin sialophosphoprotein (DSPP), another non-collagenous protein in dentin⁽⁸²⁾; whereas DMP-1 is another acidic phosphoprotein that is involved in dentin biomineralization⁽⁷⁸⁾. Although their distinct roles in the process of dentinogenesis have not yet been elucidated, DSP has been reported to be present in both young and mature odontoblasts as well as cells of the dental papilla^(62, 83-85); while DMP-1 has been reported to be secreted by more mature odontoblasts⁽⁸⁶⁾. An interesting study by D'Souza et al.⁽⁸⁷⁾ involving in situ hybridization for DMP-1 and DSPP (the DSP precursor protein) in murine molars showed that both proteins were co-expressed in young odontoblasts before the onset of mineralization; however, DMP-1 expression level was reduced after the deposition of mineral, whereas DSPP maintained its high level of expression. This

phenomenon would explain why DMP-1 was expressed in our unmineralized one-week-old organoids, but had a very low expression in the mineralized two-week-old organoids; while DSP was equally expressed at both timepoints.

Asporin is a leucine-rich protein that was first isolated from human articular cartilage^(88, 89). It was then found to be expressed in other tissues such as the aorta, uterus and bone^(89, 90). In the oral tissues, a study by Yamada et al.⁽⁶⁴⁾ reported that asporin was expressed specifically in the periodontal ligament as well as the dental follicle (the progenitor tissue for PDL, cementum and bone) and was given the alternate name of PLAP/1 (periodontal ligament associated protein 1). It was suggested in the same study that asporin is a potential negative regulator of mineralization whose function is to prevent pathological mineralization within the periodontal ligament space. Consequently, we decided to use asporin as a PDL marker to characterize the nature of the unmineralized peripheral tissue in our pinned organoids that were cultured on the PDMS/laminin substrates. At one week, there was diffuse expression of the protein marker. As a potential negative regulator of mineralization, it was understandable to find no specific localization for the protein within an organoid that is generally unmineralized. At two weeks, however, the signal was localized more toward the outer part of the organoid, including the peripheral unmineralized tissue.

For the two-week old organoids, it was interesting to see that the specific mineralization pattern was accompanied with localized protein expression. At two weeks, the DSP signal was positive in the central part of the organoid, but almost negative in the peripheral part; conversely the asporin signal was almost negative in the central part of the organoid, but positive in the peripheral part. This was highly suggestive of two different natures to the tissues within the organoid. Our results suggest that the outer cells in these organoids could potentially be differentiating into periodontal ligament-like tissue, whereas the inner cells are maintaining their

osteogenic nature and differentiating into odontoblast-like cells. This, however, raises a more important question about the nature of the so-called SCAP. Ever since their isolation and characterization in 2006^(25, 31), the cells that were found within the soft tissue pertaining to the apical end of a developing root were given the name “SCAP” as they were defined as cells derived from the “apical papilla”, which was in turn defined as an apical extension of the dental papilla tissue. It is, however, important to also understand that in an underdeveloped root that is yet to be completed along with its periodontal ligament attachment (also yet to be formed), the soft tissue at the developing root end would naturally contain both apical papilla tissue (precursor of the dentin/pulp complex of the growing root) and dental follicle tissue (precursor of the periodontium components: PDL, cementum, bone). Considering that there is no intervening tissue anatomically present between the two structures –aside from the epithelial diaphragm, which does not extend all the way between both tissues– it is very probable that this “apical papilla” tissue is in fact an ectomesenchymal structure harboring two developmental tissues: more coronally-situated dental papilla remnants and more-apically situated dental follicle remnants. When taking the anatomical continuity of both ectomesenchymal tissues into consideration, it would seem that the term “apical papilla” is imprecise, as it confines this apical soft tissue to only one tissue type. This calls for the use of a more general term such as “apical tooth germ remnant” to be inclusive of the developing tissues found within this structure and as a term that is more representative of the multifaceted capabilities of “SCAP” in driving root development. As such, this would account for the interesting localization of protein expression seen within the SCAP organoids, where it would suggest that even after enzymatic digestion of the two tissues that were isolated, the resulting heterogenous population of dental papilla and dental follicle cells were still able to undergo a process of autonomously-driven cell sorting within the scaffold-free culture to assume their native respective

positions within the organoid, with an outer dental follicle and an inner dental papilla. Hence, the asporin signal was more towards the periphery, while the DSP signal was more towards the center.

It is worth noting, however, that the area including the positive asporin staining was much thicker than the very thin rim of unmineralized tissue that was seen to encase our constructs (as shown by the ARS stains). In fact, judging by the thickness of the asporin-positive tissue, it seemed to correspond to both the outer unmineralized rim and the intermediate mineralized zone taken together. Considering that asporin has been reported as a mineralization inhibitor and PDL marker⁽⁶⁴⁾, positive expression in the area that had mineralization was not expected. This, however, falls in line with several other studies that have reported asporin expression in odontogenic tissues other than PDL such as a proteomics analysis study that revealed the presence of asporin in human dentin tissue⁽⁹¹⁾, an in situ hybridization study that reported strong expression of asporin RNA in secreting odontoblasts during matrix production⁽⁹²⁾ and finally a study involving the isolation of human DPCs by Lee et al.⁽⁹³⁾ that noted that asporin expression was expressed by early differentiating DPCs both at the gene and protein levels, where it was mostly localized to the mineralization front of the pre-dentin and during the early stages of globular calcification in pre-dentin. Interestingly, the same study also showed that asporin knock-down suppressed DPC mineralization. As such, asporin may be a multifaceted molecule that plays a paradoxical role in initiating mineralization, but also preventing excessive mineral deposition, and therefore is usually found around interfaces between mineralized and unmineralized tissue, including the pre-dentin-dentin interface and the bone-PDL-cementum interface.

Therefore, possible steps for future work can include using marker proteins that are more specific for dental follicle or periodontal ligament tissue, such as F-spondin or Tenascin-N respectively^(94, 95). Also comparing tissue patterning and protein expression profiles in SCAP

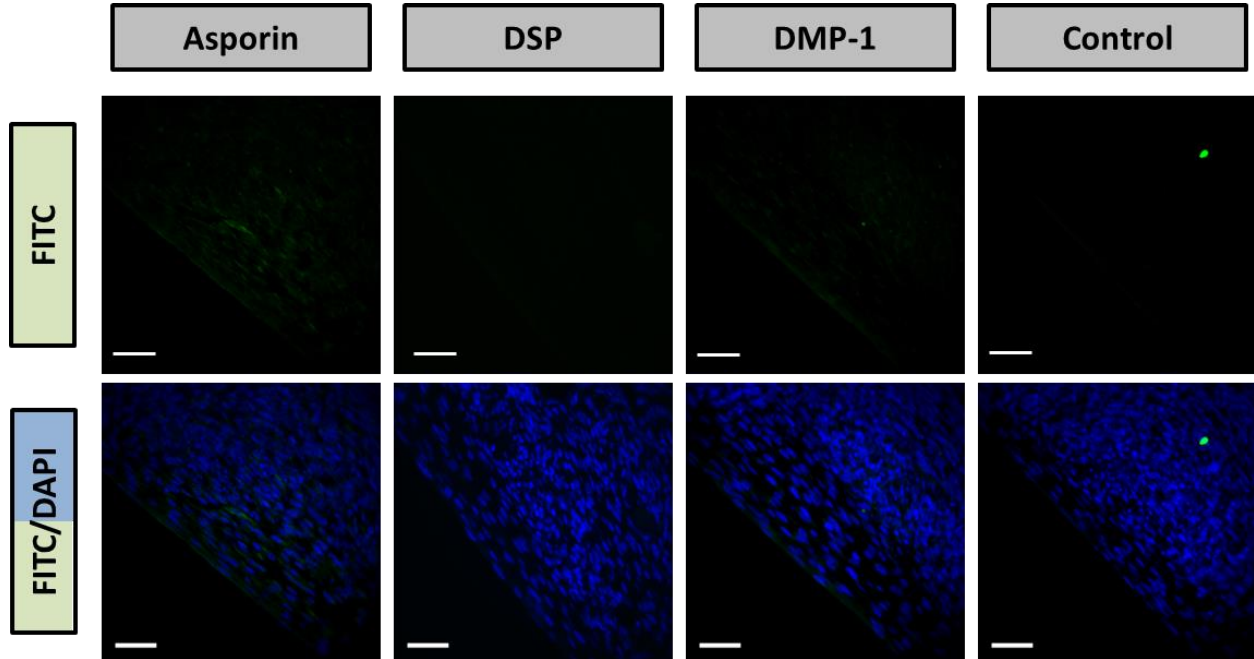
organoids with those of organoids from other cell populations (such as DPCs or PDLCs) can help us better understand how each tissue is different. Lastly, *in vivo* studies can be conducted to evaluate how SCAP organoids would mature *in vivo* and how well they would function under masticatory load.

Limitations to this study included difficulties in getting a uniformly confluent SCAP cell sheet to form on the PDMS/laminin substrates, where the plated cells would often form discrete clumps of cell aggregates without forming a uniform cell sheet. This phenomenon was noted only in SCAP (and not in DPCs), and only on the PDMS/laminin substrates (not on TCP). This suggests a uniqueness regarding how specifically SCAP is interacting with the PDMS/laminin substrate. This seems to be related to the phenomenon of integrin clustering which occurs during adhesion between cells and the underlying substrate, where a repulsive layer is hypothetically created between the membrane of the cell and the underlying substrate (potentially because of electrostatic repulsion of charged surfaces) and the thickness of this layer would dictate the strength of the attractive interactions between adjacent integrin receptors⁽⁹⁶⁾. Therefore, possible future modifications to avoid this could include plating the cells on the PDMS/laminin substrates at a lower density to reduce these attractive interactions. Another possible approach would be to give a double coating of laminin (a single coating which when dry, would be followed by a second coating) to improve cell-substrate contact and minimize the repulsive layer, thereby decreasing the attraction between adjacent integrin receptors and hence avoiding excessive focal adhesions in culture. Another limitation to the study was the limited number of replicates, which included cells from only one patient. Consequently, more experiments with cells derived from different patients will need to be done to test the reproducibility of the results.

6.0 CONCLUSION

In conclusion, our study has shown that scaffold-free engineered SCAP tissue can self-assemble into a multi-tissue organoid, with a mineralization pattern similar to that of a tooth root, with an outer unmineralized peripheral tissue (resembling unmineralized PDL), an intermediate mineralized tissue (resembling cementum/dentin) and innermost unmineralized tissue (resembling pulp). Our study also puts forth culture substrate and final organoid geometry as potential factors that can have dramatic effects on tissue patterning. Our study also poses important questions about the identity of the apical papilla tissue and the potential dual nature of the ectomesenchymal tissues it harbors. This can shed new light on the complexity of this tissue and the potential roles it can play in forming the diverse tissues of a developing root.

Appendix A Protein expression in SCAP organoids at one week



Appendix Figure 1 Immunofluorescent staining of SCAP organoids at one week was performed to detect localization of DSP, DMP-1 and asporin expression. 50% of the organoids at one week showed little-to-no protein expression. {Scale bar = 50 μ m}

Appendix B Implanting the SCAP organoids in vivo

A pilot experiment was performed to assess the in vivo maturation of one-week-old SCAP organoids after 4 weeks of subcutaneous and subrenal capsule implantation.

Appendix B.1 Materials and Methods

Immunocompromised BALB/c nude mice aged 6-7 weeks were purchased from Charles River Laboratories (USA) and were housed under standard conditions of alternate light and dark cycle. The surgical procedure was approved by the Institutional Animal Care and Use Committee (IACUC) University of Pittsburgh. Before beginning the surgical procedure, the mouse was placed in an anesthetic induction chamber for isoflurane anesthesia at ~3-6%. When the animal had stopped moving, the animal was put on a nose cone for maintaining the anesthesia during the surgical procedure at ~2-3%. The surgical site was prepared by cleaning with 70% alcohol wipes and 10% povidone-Iodine solution swab sticks.

Subcutaneous implantation: An ~1 cm skin incision was made over the dorsal surface of the mice using fine scissors, followed by separating the dermis from the body wall on one side of the incision. Using fine forceps, the constructs were gently placed in the pouch created between the dermis and the body wall. Up to 4 skin incisions and pouches were created in each animal, each occupying one corner of the dorsal surface of the animal. The incisions were closed using wound clips.

Subrenal capsule implantation: An ~2 cm dorsal midline skin incision was made, followed by separating the dermis from the body wall on the left side of the incision (for unilateral grafting). The mouse was placed in a slight lateral position for the location of the left kidney to be visualized through the muscle wall. The muscle wall overlying the visualized kidney was elevated using fine forceps and a 1cm incision was done in the overlying muscle wall, in a direction parallel to the spine. The initial incision was then made wider, by placing the scissors in the incision and then gently opening them. The kidney was then exteriorized by applying gentle pressure on the muscle wall on either side of the kidney. Hydration of the exteriorized kidney was maintained by frequently applying sterile saline. The kidney capsule was very gently lifted from the kidney parenchyma, using fine #5 forceps, and with the use of fine scissors, a 2-4mm cut was made in the capsule. Using a glass Pasteur pipette (whose tip had been fire-polished over a Bunsen burner to form a curved rounded tip), a small pouch was created by gently inserting the pipette tip in a tangential direction between the capsule and the underlying kidney parenchyma. The pipette tip was then used to place the construct in the created pouch. Up to 3 pouches were created in the kidney of each animal, each holding a separate construct. When done, the kidney was put back in the body cavity by gently lifting the ends of the incised muscle wall on either side of incision. The muscle wall incision was closed using a single suture (3-0 vicryl suture), and the overlying skin incision was closed using wound clips.

After the surgery, the mice were given a subcutaneous Buprenorphine hydrochloride analgesic injection (Torbugesic; Covetrus, USA), as the primary post-operative pain reliever with a dosage of 0.05-0.1 mg/KG. The animals were then placed over a warm-water-filled glove and allowed to regain consciousness. They were then housed with access to food and water. Each two mice were given one Carprofen tablet per day (Rimadyl; Bio-serv, USA), containing 2mg/tablet,

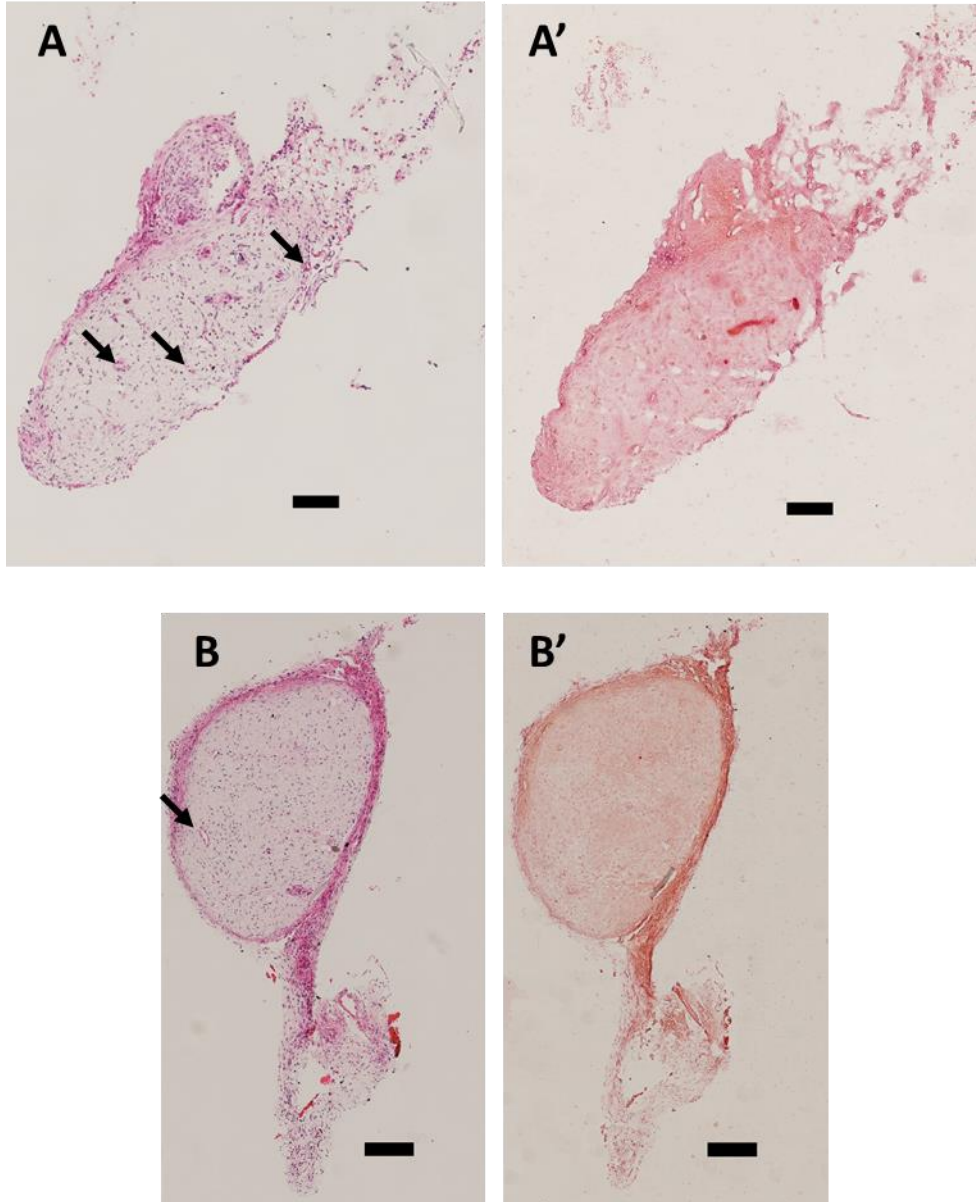
for three consecutive days. The mice were monitored and weighed every day over a period of one week following the surgery to ensure that the animals were mobile and not lethargic and to observe for any loss in weight.

One round of animal surgery was done, where 12 constructs were implanted into two animals: each receiving 2 constructs in the subrenal capsule and 4 constructs subcutaneously.

Appendix B.2 Results

Histological characterization for tissue morphology and mineral deposition was performed for the explants. H&E images of the explants showed that the cell/ECM ratio was reduced (as compared to the in vitro organoids) and blood vessels were seen within the explanted tissue (arrows in Appendix Fig.2A, B). ARS staining was negative for the explanted organoids (Appendix Fig.2A', B').

This experiment will need to be repeated for more samples at one and two weeks to assess tissue maturation and patterning within the organoids in vivo, as well as to compare the two implantation sites for potential differences in their effect on overall maturation of the organoids.



Appendix Figure 2 Histological analysis of SCAP explants after 4 weeks of in vivo implantation. (A, A'): Subrenal capsule explants stained with H&E and ARS respectively. (B, B'): Subcutaneous explants stained with H&E and ARS respectively {Arrows pointing to blood vessels; Scale bar = 200 μ m}

Bibliography

- 1.Nanci A, TenCate AR. Ten Cate's oral histology : development, structure, and function2018.
- 2.Britannica E. Cross section of an adult human molar. Copyright © 2013 Encyclopædia Britannica, Inc.
- 3.Calvo SPLJ. Light micrograph of a developing tooth in the bell stage of odontogenesis. .
- 4.Lin JC, Lu JX, Zeng Q, Zhao W, Li WQ, Ling JQ. Comparison of mineral trioxide aggregate and calcium hydroxide for apexification of immature permanent teeth: A systematic review and meta-analysis. *J Formos Med Assoc.* 2016;115(7):523-30.
- 5.Silujjai J, Linsuwanont P. Treatment Outcomes of Apexification or Revascularization in Nonvital Immature Permanent Teeth: A Retrospective Study. *J Endod.* 2017;43(2):238-45.
- 6.Namour M, Theys S. Pulp revascularization of immature permanent teeth: a review of the literature and a proposal of a new clinical protocol. *ScientificWorldJournal.* 2014;2014:737503.
- 7.Banchs F, Trope M. Revascularization of immature permanent teeth with apical periodontitis: new treatment protocol? *J Endod.* 2004;30(4):196-200.
- 8.Reynolds K, Johnson JD, Cohenca N. Pulp revascularization of necrotic bilateral bicuspid using a modified novel technique to eliminate potential coronal discoloration: a case report. *Int Endod J.* 2009;42(1):84-92.
- 9.Thomson A, Kahler B. Regenerative endodontics--biologically-based treatment for immature permanent teeth: a case report and review of the literature. *Aust Dent J.* 2010;55(4):446-52.
- 10.Chen YP, Jovani-Sancho Mdel M, Sheth CC. Is revascularization of immature permanent teeth an effective and reproducible technique? *Dent Traumatol.* 2015;31(6):429-36.
- 11.Shimizu E, Ricucci D, Albert J, Alobaid AS, Gibbs JL, Huang GT, et al. Clinical, radiographic, and histological observation of a human immature permanent tooth with chronic apical abscess after revitalization treatment. *J Endod.* 2013;39(8):1078-83.
- 12.Lei L, Chen Y, Zhou R, Huang X, Cai Z. Histologic and Immunohistochemical Findings of a Human Immature Permanent Tooth with Apical Periodontitis after Regenerative Endodontic Treatment. *J Endod.* 2015;41(7):1172-9.
- 13.Becerra P, Ricucci D, Loghin S, Gibbs JL, Lin LM. Histologic study of a human immature permanent premolar with chronic apical abscess after revascularization/revitalization. *J Endod.* 2014;40(1):133-9.

14. Digka A, Sakka D, Lyroudia K. Histological assessment of human regenerative endodontic procedures (REP) of immature permanent teeth with necrotic pulp/apical periodontitis: A systematic review. *Aust Endod J.* 2020;46(1):140-53.
15. Mao JJ, Kim SG, Zhou J, Ye L, Cho S, Suzuki T, et al. Regenerative endodontics: barriers and strategies for clinical translation. *Dent Clin North Am.* 2012;56(3):639-49.
16. Lin LM, Kahler B. A review of regenerative endodontics: current protocols and future directions. *J Istanbul Univ Fac Dent.* 2017;51(3 Suppl 1):S41-S51.
17. Siddiqui SH, Mohamed AN. Calcific Metamorphosis: A Review. *Int J Health Sci (Qassim).* 2016;10(3):437-42.
18. McCabe PS, Dummer PM. Pulp canal obliteration: an endodontic diagnosis and treatment challenge. *Int Endod J.* 2012;45(2):177-97.
19. Song M, Cao Y, Shin SJ, Shon WJ, Chugal N, Kim RH, et al. Revascularization-associated Intracanal Calcification: Assessment of Prevalence and Contributing Factors. *J Endod.* 2017;43(12):2025-33.
20. Kahler B, Kahler SL, Lin LM. Revascularization-associated Intracanal Calcification: A Case Report with an 8-year Review. *J Endod.* 2018;44(12):1792-5.
21. Gronthos S, Mankani M, Brahim J, Robey PG, Shi S. Postnatal human dental pulp stem cells (DPSCs) in vitro and in vivo. *Proc Natl Acad Sci U S A.* 2000;97(25):13625-30.
22. Miura M, Gronthos S, Zhao M, Lu B, Fisher LW, Robey PG, et al. SHED: stem cells from human exfoliated deciduous teeth. *Proc Natl Acad Sci U S A.* 2003;100(10):5807-12.
23. Seo BM, Miura M, Gronthos S, Bartold PM, Batouli S, Brahim J, et al. Investigation of multipotent postnatal stem cells from human periodontal ligament. *Lancet.* 2004;364(9429):149-55.
24. Matsubara T, Suardita K, Ishii M, Sugiyama M, Igarashi A, Oda R, et al. Alveolar bone marrow as a cell source for regenerative medicine: differences between alveolar and iliac bone marrow stromal cells. *J Bone Miner Res.* 2005;20(3):399-409.
25. Sonoyama W, Liu Y, Fang D, Yamaza T, Seo BM, Zhang C, et al. Mesenchymal stem cell-mediated functional tooth regeneration in swine. *PLoS One.* 2006;1:e79.
26. Ikeda E, Yagi K, Kojima M, Yagyuu T, Ohshima A, Sobajima S, et al. Multipotent cells from the human third molar: feasibility of cell-based therapy for liver disease. *Differentiation.* 2008;76(5):495-505.

27. Zhang Q, Shi S, Liu Y, Uyanne J, Shi Y, Shi S, et al. Mesenchymal stem cells derived from human gingiva are capable of immunomodulatory functions and ameliorate inflammation-related tissue destruction in experimental colitis. *J Immunol.* 2009;183(12):7787-98.
28. Batouli S, Miura M, Brahim J, Tsutsui TW, Fisher LW, Gronthos S, et al. Comparison of stem-cell-mediated osteogenesis and dentinogenesis. *J Dent Res.* 2003;82(12):976-81.
29. Takeda T, Tezuka Y, Horiuchi M, Hosono K, Iida K, Hatakeyama D, et al. Characterization of dental pulp stem cells of human tooth germs. *J Dent Res.* 2008;87(7):676-81.
30. Syed-Picard FN, Ray HL, Jr., Kumta PN, Sfeir C. Scaffoldless tissue-engineered dental pulp cell constructs for endodontic therapy. *J Dent Res.* 2014;93(3):250-5.
31. Sonoyama W, Liu Y, Yamaza T, Tuan RS, Wang S, Shi S, et al. Characterization of the apical papilla and its residing stem cells from human immature permanent teeth: a pilot study. *J Endod.* 2008;34(2):166-71.
32. Kang J, Fan W, Deng Q, He H, Huang F. Stem Cells from the Apical Papilla: A Promising Source for Stem Cell-Based Therapy. *Biomed Res Int.* 2019;2019:6104738.
33. Huang GT, Sonoyama W, Liu Y, Liu H, Wang S, Shi S. The hidden treasure in apical papilla: the potential role in pulp/dentin regeneration and bioroot engineering. *J Endod.* 2008;34(6):645-51.
34. Nada OA, El Backly RM. Stem Cells From the Apical Papilla (SCAP) as a Tool for Endogenous Tissue Regeneration. *Front Bioeng Biotechnol.* 2018;6:103.
35. Ovsianikov A, Khademhosseini A, Mironov V. The Synergy of Scaffold-Based and Scaffold-Free Tissue Engineering Strategies. *Trends Biotechnol.* 2018;36(4):348-57.
36. Alblawi A, Ranjani AS, Yasmin H, Gupta S, Bit A, Rahimi-Gorji M. Scaffold-free: A developing technique in field of tissue engineering. *Comput Methods Programs Biomed.* 2020;185:105148.
37. Alghuwainem A, Alshareeda AT, Alsowayan B. Scaffold-Free 3-D Cell Sheet Technique Bridges the Gap between 2-D Cell Culture and Animal Models. *Int J Mol Sci.* 2019;20(19).
38. Lee JK, Link JM, Hu JCY, Athanasiou KA. The Self-Assembling Process and Applications in Tissue Engineering. *Cold Spring Harb Perspect Med.* 2017;7(11).
39. Shimizu T, Sekine H, Yamato M, Okano T. Cell sheet-based myocardial tissue engineering: new hope for damaged heart rescue. *Curr Pharm Des.* 2009;15(24):2807-14.
40. Saito J, Yokoyama U, Nakamura T, Kanaya T, Ueno T, Naito Y, et al. Scaffold-free tissue-engineered arterial grafts derived from human skeletal myoblasts. *Artif Organs.* 2021.

41. Nishida K, Yamato M, Hayashida Y, Watanabe K, Yamamoto K, Adachi E, et al. Corneal reconstruction with tissue-engineered cell sheets composed of autologous oral mucosal epithelium. *N Engl J Med*. 2004;351(12):1187-96.
42. Shimizu H, Ohashi K, Utoh R, Ise K, Gotoh M, Yamato M, et al. Bioengineering of a functional sheet of islet cells for the treatment of diabetes mellitus. *Biomaterials*. 2009;30(30):5943-9.
43. Ohki T, Yamato M, Murakami D, Takagi R, Yang J, Namiki H, et al. Treatment of oesophageal ulcerations using endoscopic transplantation of tissue-engineered autologous oral mucosal epithelial cell sheets in a canine model. *Gut*. 2006;55(12):1704-10.
44. Kanzaki M, Yamato M, Yang J, Sekine H, Takagi R, Isaka T, et al. Functional closure of visceral pleural defects by autologous tissue engineered cell sheets. *Eur J Cardiothorac Surg*. 2008;34(4):864-9.
45. Iwata T, Yamato M, Tsuchioka H, Takagi R, Mukobata S, Washio K, et al. Periodontal regeneration with multi-layered periodontal ligament-derived cell sheets in a canine model. *Biomaterials*. 2009;30(14):2716-23.
46. Jensen C, Teng Y. Is It Time to Start Transitioning From 2D to 3D Cell Culture? *Front Mol Biosci*. 2020;7:33.
47. Gao X, Wu Y, Liao L, Tian W. Oral Organoids: Progress and Challenges. *J Dent Res*. 2021:22034520983808.
48. de Souza N. Organoids. *Nature Methods*. 2018;15(1):23-.
49. Hosseini ZF, Nelson DA, Moskwa N, Larsen M. Generating Embryonic Salivary Gland Organoids. *Curr Protoc Cell Biol*. 2019;83(1):e76.
50. Tanaka J, Ogawa M, Hojo H, Kawashima Y, Mabuchi Y, Hata K, et al. Generation of orthotopically functional salivary gland from embryonic stem cells. *Nat Commun*. 2018;9(1):4216.
51. Nakao K, Morita R, Saji Y, Ishida K, Tomita Y, Ogawa M, et al. The development of a bioengineered organ germ method. *Nat Methods*. 2007;4(3):227-30.
52. Ono M, Oshima M, Ogawa M, Sonoyama W, Hara ES, Oida Y, et al. Practical whole-tooth restoration utilizing autologous bioengineered tooth germ transplantation in a postnatal canine model. *Sci Rep*. 2017;7:44522.
53. Kim EJ, Yoon KS, Arakaki M, Otsu K, Fukumoto S, Harada H, et al. Effective Differentiation of Induced Pluripotent Stem Cells Into Dental Cells. *Dev Dyn*. 2019;248(1):129-39.
54. Cai J, Zhang Y, Liu P, Chen S, Wu X, Sun Y, et al. Generation of tooth-like structures from integration-free human urine induced pluripotent stem cells. *Cell Regen*. 2013;2(1):6.

55. Rosowski J, Braunig J, Amler AK, Strietzel FP, Lauster R, Rosowski M. Emulating the early phases of human tooth development in vitro. *Sci Rep*. 2019;9(1):7057.
56. Syed-Picard FN, Jayaraman T, Lam RS, Beniash E, Sfeir C. Osteoinductivity of calcium phosphate mediated by connexin 43. *Biomaterials*. 2013;34(15):3763-74.
57. Basu A, Rothermund K, Ahmed MN, Syed-Picard FN. Self-Assembly of an Organized Cementum-Periodontal Ligament-Like Complex Using Scaffold-Free Tissue Engineering. *Front Physiol*. 2019;10:422.
58. Cowin SC. How is a tissue built? *J Biomech Eng*. 2000;122(6):553-69.
59. Takebe T, Wells JM. Organoids by design. *Science*. 2019;364(6444):956-9.
60. Vogel V, Sheetz M. Local force and geometry sensing regulate cell functions. *Nat Rev Mol Cell Biol*. 2006;7(4):265-75.
61. Begue-Kirn C, Krebsbach PH, Bartlett JD, Butler WT. Dentin sialoprotein, dentin phosphoprotein, enamelysin and ameloblastin: tooth-specific molecules that are distinctively expressed during murine dental differentiation. *Eur J Oral Sci*. 1998;106(5):963-70.
62. Ritchie HH, Berry JE, Somerman MJ, Hanks CT, Bronckers AL, Hotton D, et al. Dentin sialoprotein (DSP) transcripts: developmentally-sustained expression in odontoblasts and transient expression in pre-ameloblasts. *Eur J Oral Sci*. 1997;105(5 Pt 1):405-13.
63. Ching HS, Luddin N, Rahman IA, Ponnuraj KT. Expression of Odontogenic and Osteogenic Markers in DPSCs and SHED: A Review. *Curr Stem Cell Res Ther*. 2017;12(1):71-9.
64. Yamada S, Tomoeda M, Ozawa Y, Yoneda S, Terashima Y, Ikezawa K, et al. PLAP-1/asporin, a novel negative regulator of periodontal ligament mineralization. *J Biol Chem*. 2007;282(32):23070-80.
65. De Pieri A, Rochev Y, Zeugolis DI. Scaffold-free cell-based tissue engineering therapies: advances, shortfalls and forecast. *NPJ Regen Med*. 2021;6(1):18.
66. Zhou C, Zhang D, Du W, Zou J, Li X, Xie J. Substrate mechanics dictate cell-cell communication by gap junctions in stem cells from human apical papilla. *Acta Biomater*. 2020;107:178-93.
67. Virjula S, Zhao F, Leivo J, Vanhatupa S, Kreutzer J, Vaughan TJ, et al. The effect of equiaxial stretching on the osteogenic differentiation and mechanical properties of human adipose stem cells. *J Mech Behav Biomed Mater*. 2017;72:38-48.
68. Witkowska-Zimny M, Walenko K, Wrobel E, Mrowka P, Mikulska A, Przybylski J. Effect of substrate stiffness on the osteogenic differentiation of bone marrow stem cells and bone-derived cells. *Cell Biol Int*. 2013;37(6):608-16.

69. Zhao W, Li X, Liu X, Zhang N, Wen X. Effects of substrate stiffness on adipogenic and osteogenic differentiation of human mesenchymal stem cells. *Mater Sci Eng C Mater Biol Appl*. 2014;40:316-23.
70. Liu N, Zhou M, Zhang Q, Yong L, Zhang T, Tian T, et al. Effect of substrate stiffness on proliferation and differentiation of periodontal ligament stem cells. *Cell Prolif*. 2018;51(5):e12478.
71. Liu N, Zhou M, Zhang Q, Zhang T, Tian T, Ma Q, et al. Stiffness regulates the proliferation and osteogenic/odontogenic differentiation of human dental pulp stem cells via the WNT signalling pathway. *Cell Prolif*. 2018;51(2):e12435.
72. Zhou C, Zhang D, Zou J, Li X, Zou S, Xie J. Substrate Compliance Directs the Osteogenic Lineages of Stem Cells from the Human Apical Papilla via the Processes of Mechanosensing and Mechanotransduction. *ACS Appl Mater Interfaces*. 2019;11(29):26448-59.
73. Shen T, Qiu L, Chang H, Yang Y, Jian C, Xiong J, et al. Cyclic tension promotes osteogenic differentiation in human periodontal ligament stem cells. *Int J Clin Exp Pathol*. 2014;7(11):7872-80.
74. Friedl G, Schmidt H, Rehak I, Kostner G, Schauenstein K, Windhager R. Undifferentiated human mesenchymal stem cells (hMSCs) are highly sensitive to mechanical strain: transcriptionally controlled early osteo-chondrogenic response in vitro. *Osteoarthritis Cartilage*. 2007;15(11):1293-300.
75. Yang X, Gong P, Lin Y, Zhang L, Li X, Yuan Q, et al. Cyclic tensile stretch modulates osteogenic differentiation of adipose-derived stem cells via the BMP-2 pathway. *Arch Med Sci*. 2010;6(2):152-9.
76. Retrouvey J-M, Goldberg M, Schwartz S. Chapter 5 - Dental Development and Maturation, from the Dental Crypt to the Final Occlusion. In: Glorieux FH, Pettifor JM, Jüppner H, editors. *Pediatric Bone (Second Edition)*. San Diego: Academic Press; 2012. p. 83-108.
77. Feng JQ, Ward LM, Liu S, Lu Y, Xie Y, Yuan B, et al. Loss of DMP1 causes rickets and osteomalacia and identifies a role for osteocytes in mineral metabolism. *Nat Genet*. 2006;38(11):1310-5.
78. Ye L, MacDougall M, Zhang S, Xie Y, Zhang J, Li Z, et al. Deletion of dentin matrix protein-1 leads to a partial failure of maturation of predentin into dentin, hypomineralization, and expanded cavities of pulp and root canal during postnatal tooth development. *J Biol Chem*. 2004;279(18):19141-8.
79. Oya K, Ishida K, Nishida T, Sato S, Kishino M, Hirose K, et al. Immunohistochemical analysis of dentin matrix protein 1 (Dmp1) phosphorylation by Fam20C in bone: implications for the induction of biomineralization. *Histochem Cell Biol*. 2017;147(3):341-51.

80. Qin C, Brunn JC, Cadena E, Ridall A, Butler WT. Dentin sialoprotein in bone and dentin sialophosphoprotein gene expressed by osteoblasts. *Connect Tissue Res.* 2003;44 Suppl 1:179-83.
81. Qin C, Brunn JC, Cadena E, Ridall A, Tsujigiwa H, Nagatsuka H, et al. The expression of dentin sialophosphoprotein gene in bone. *J Dent Res.* 2002;81(6):392-4.
82. MacDougall M, Simmons D, Luan X, Nydegger J, Feng J, Gu TT. Dentin phosphoprotein and dentin sialoprotein are cleavage products expressed from a single transcript coded by a gene on human chromosome 4. Dentin phosphoprotein DNA sequence determination. *J Biol Chem.* 1997;272(2):835-42.
83. Bronckers AL, D'Souza RN, Butler WT, Lyaruu DM, van Dijk S, Gay S, et al. Dentin sialoprotein: biosynthesis and developmental appearance in rat tooth germs in comparison with amelogenins, osteocalcin and collagen type-I. *Cell Tissue Res.* 1993;272(2):237-47.
84. Butler WT. Dentin matrix proteins. *Eur J Oral Sci.* 1998;106 Suppl 1:204-10.
85. Boskey A, Spevak L, Tan M, Doty SB, Butler WT. Dentin sialoprotein (DSP) has limited effects on in vitro apatite formation and growth. *Calcif Tissue Int.* 2000;67(6):472-8.
86. George A, Silberstein R, Veis A. In situ hybridization shows Dmp1 (AG1) to be a developmentally regulated dentin-specific protein produced by mature odontoblasts. *Connect Tissue Res.* 1995;33(1-3):67-72.
87. D'Souza RN, Cavender A, Sunavala G, Alvarez J, Ohshima T, Kulkarni AB, et al. Gene expression patterns of murine dentin matrix protein 1 (Dmp1) and dentin sialophosphoprotein (DSPP) suggest distinct developmental functions in vivo. *J Bone Miner Res.* 1997;12(12):2040-9.
88. Henry SP, Takanosu M, Boyd TC, Mayne PM, Eberspaecher H, Zhou W, et al. Expression pattern and gene characterization of asporin, a newly discovered member of the leucine-rich repeat protein family. *J Biol Chem.* 2001;276(15):12212-21.
89. Lorenzo P, Aspberg A, Onnerfjord P, Bayliss MT, Neame PJ, Heinegard D. Identification and characterization of asporin, a novel member of the leucine-rich repeat protein family closely related to decorin and biglycan. *J Biol Chem.* 2001;276(15):12201-11.
90. Boskey AL, Robey PG. Chapter 11 - The Regulatory Role of Matrix Proteins in Mineralization of Bone. In: Marcus R, Feldman D, Dempster DW, Luckey M, Cauley JA, editors. *Osteoporosis (Fourth Edition)*. San Diego: Academic Press; 2013. p. 235-55.
91. Park ES, Cho HS, Kwon TG, Jang SN, Lee SH, An CH, et al. Proteomics analysis of human dentin reveals distinct protein expression profiles. *J Proteome Res.* 2009;8(3):1338-46.
92. Wurtz T, Houari S, Mauro N, MacDougall M, Peters H, Berdal A. Fluoride at non-toxic dose affects odontoblast gene expression in vitro. *Toxicology.* 2008;249(1):26-34.

93.Lee EH, Park HJ, Jeong JH, Kim YJ, Cha DW, Kwon DK, et al. The role of asporin in mineralization of human dental pulp stem cells. *J Cell Physiol.* 2011;226(6):1676-82.

94.Nishida E, Sasaki T, Ishikawa SK, Kosaka K, Aino M, Noguchi T, et al. Transcriptome database KK-Periome for periodontal ligament development: expression profiles of the extracellular matrix genes. *Gene.* 2007;404(1-2):70-9.

95.Saito M, Nishida E, Yoneda T. Comprehensive Analysis of Tissue-specific Markers Involved in Periodontal Ligament Development. *Journal of Oral Biosciences.* 2008;50(3):175-82.

96.Yuan H, Gao H. On the mechanics of integrin clustering during cell-substrate adhesion. *Acta Mechanica Solida Sinica.* 2012;25(5):467-72.